# HapMap scanning of novel human minor histocompatibility antigens

*Michi Kamei,[1,2] *Yasuhito Nannya,[3-5] Hiroki Torikai,[1] Takakazu Kawase,[1,6] Kenjiro Taura,[7] Yoshihiro Inamoto,[8] Taro Takahashi,[8] Makoto Yazaki,[9] Satoko Morishima,[1] Kunio Tsujimura,[10] Koichi Miyamura,[5,8] Tetsuya Ito,[2] Hajime Togari,[2] Stanley R. Riddell,[11] Yoshihisa Kodera,[5,8] Yasuo Morishima,[5,12] Toshitada Takahashi,[13] Kiyotaka Kuzushima,[1] †Seishi Ogawa,[4,5] and †Yoshiki Akatsuka[1,5]

[1]Division of Immunology, Aichi Cancer Center Research Institute, Nagoya, Japan; [2]Department of Pediatrics and Neonatology, Nagoya City University, Graduate School of Medical Science, Nagoya, Japan; [3]Department of Hematology/Oncology and [4]The 21st Century Center of Excellence (COE) Program, Graduate School of Medicine, University of Tokyo, Tokyo, Japan; [5]Core Research for Evolutional Science and Technology, Japan Science and Technology Agency, Saitama, Japan; [6]Division of Epidemiology and Prevention, Aichi Cancer Center Research Institute, Nagoya, Japan; [7]Department of Information and Communication Engineering, Graduate School of Information Science, University of Tokyo, Tokyo, Japan; [8]Department of Hematology, Japanese Red Cross Nagoya First Hospital, Nagoya, Japan; [9]Department of Pediatrics, Higashi Municipal Hospital of Nagoya, Nagoya, Japan; [10]Department of Infectious Diseases, Hamamatsu University School of Medicine, Hamamatsu, Japan; [11]Program in Immunology, Clinical Research Division, Fred Hutchinson Cancer Research Center, Seattle, WA; [12]Department of Hematology and Cell Therapy, Aichi Cancer Center Central Hospital, Nagoya, Japan; and [13]Aichi Comprehensive Health Science Center, Aichi Health Promotion Foundation, Chita-gun, Japan

**Minor histocompatibility antigens (mHags) are molecular targets of alloimmunity associated with hematopoietic stem cell transplantation (HSCT) and involved in graft-versus-host disease, but they also have beneficial antitumor activity. mHags are typically defined by host SNPs that are not shared by the donor and are immunologically recognized by cytotoxic T cells isolated from post-HSCT patients. However, the number of molecularly identified mHags is still too small to allow prospective studies of their clinical importance in transplantation medicine, mostly due to the lack of an efficient method for isolation. Here we show that when combined with conventional immunologic assays, the large data set from the International HapMap Project can be directly used for genetic mapping of novel mHags. Based on the immunologically determined mHag status in HapMap panels, a target mHag locus can be uniquely mapped through whole genome association scanning taking advantage of the unprecedented resolution and power obtained with more than 3 000 000 markers. The feasibility of our approach could be supported by extensive simulations and further confirmed by actually isolating 2 novel mHags as well as 1 previously identified example. The HapMap data set represents an invaluable resource for investigating human variation, with obvious applications in genetic mapping of clinically relevant human traits. (Blood. 2009;113:5041-5048)**

## Introduction

The antitumor activity of allogeneic hematopoietic stem cell transplantation (HSCT), which is a curative treatment for many patients with hematologic malignancies, is mediated in part by immune responses that are elicited as a consequence of incompatibility in genetic polymorphisms between the donor and the recipient.[1,2] Analysis of patients treated for posttransplantation relapse with donor lymphocytes has shown tumor regression to be correlated with expansion of cytotoxic T lymphocytes (CTLs) specific for hematopoiesis-restricted minor histocompatibility antigens (mHags).[3,4] mHags are peptides, presented by major histocompatibility complex (MHC) molecules, derived from intracellular proteins that differ between donor and recipient due mostly to single nucleotide polymorphisms (SNPs) or copy number variations (CNVs).[1,2,5] Identification and characterization of mHags that are specifically expressed in hematopoietic but not in other normal tissues could contribute to graft-versus-leukemia/lymphoma (GVL) effects, while minimizing unfavorable graft-versus-host disease, one of the most serious complications of allo-HSCT.[1,2] Unfortunately, however, efforts to prospectively target mHags to invoke T cell–mediated selective GVL effects have been hampered by the scarcity of eligible mHags, largely due to the lack of efficient methods for mapping the relevant genetic loci. Several methods have been developed to identify mHags, including peptide elution from MHC,[6,7] cDNA expression cloning,[8,9] and linkage analysis.[3,10] We have recently reported a novel genetic method that combines whole genome association scanning with conventional chromium release cytotoxicity assays (CRAs). With this approach the genetic loci of the mHag gene recognized by a given CTL clone can be precisely identified using SNP array analysis of pooled DNA generated from immortalized lymphoblastoid cell lines (LCLs) that are immunophenotyped into $mHag^+$ and $mHag^-$ groups by CRA.[11] The mapping resolution has now been improved from several Mb for conventional linkage analysis to an average haplotype block size of less than 100 kb,[12] usually containing a handful of candidate genes. Nevertheless, it still requires laborious DNA pooling and scanning of SNP arrays with professional expertise for individual

Submitted July 29, 2008; accepted August 27, 2008. Prepublished online as *Blood* First Editon paper, September 22, 2008; DOI 10.1182/blood-2008-07-171678.

*M.K. and Y.N. are first coauthors and contributed equally to this work.

†S.O. and Y.A. are senior coauthors.

An Inside *Blood* analysis of this article appears at the front of this issue.

The online version of this article contains a data supplement.

The publication costs of this article were defrayed in part by page charge payment. Therefore, and solely to indicate this fact, this article is hereby marked "advertisement" in accordance with 18 USC section 1734.

CTLs.[11] To circumvent these drawbacks, we have sought to take advantage of publicly available HapMap resources. Here, we describe a powerful approach for rapidly identifying mHAg loci using a large genotyping data set and LCLs from the International HapMap Project for genome-wide association analysis.[13-15]

## Methods

### Cell lines and CTL clones

The HapMap LCL samples were purchased from the Coriell Institute (Camden, NJ). All LCLs were maintained in RPMI1640 supplemented with 10% fetal calf serum, 2 mM L-glutamine, and 1 mM sodium pyruvate. Because the recognition of a mHag requires presentation on a particular type of HLA molecule, the LCLs were stably transduced with a retroviral vector encoding the restriction HLA cDNA for a given CTL clone when necessary.[16]

CTL lines were generated from recipient peripheral blood mononuclear cells obtained after transplantation by stimulation with those harvested before HSCT after irradiation (33 Gy), and thereafter stimulated weekly in RPMI 1640 supplemented with 10% pooled human serum and 2 mM L-glutamine. Recombinant human inerleukin-2 was added on days 1 and 5 after the second and third stimulations. CTL clones were isolated by standard limiting dilution and expanded as previously described.[10,17] HLA restriction was determined by conventional CRAs against a panel of LCLs sharing HLA alleles with the CTLs. All clinical samples were collected based on a protocol approved by the Institutional Review Board Committee at Aichi Cancer Center and the University of Tokyoand after written informed consent was obtained in accordance with the Declaration of Helsinki.

### Immunophenotyping of HapMap LCLs and high-density genome-wide scanning of mHag loci

Case ($mHag^+$) - control ($mHag^-$) LCL panels were generated by screening corresponding restriction HLA-transduced CHB and JPT HapMap LCL panels with each CTL clone using CRAs. Briefly, target cells were labeled with 0.1 mCi of $^{51}Cr$ for 2 hours, and $10^3$ target cells per well were mixed with CTL at a predetermined E/T ratio in a standard 4-hour CRA. All assays were performed at least in duplicate. The percent specific lysis was calculated by ((Experimental cpm - Spontaneous cpm) / (Maximum cpm - Spontaneous cpm)) × 100. After normalization by dividing their percent specific lysis values by that of positive control LCL (typically recipient-derived LCL corresponding to individual CTL clones), the mHag status of each HapMap LCL was defined as positive, negative, or undetermined.

To identify mHag loci, we performed association tests for all the Phase II HapMap SNPs, by calculating $\chi^2$ test statistics based on 2 × 2 contingency tables with regard to the mHag status as measured by CRA and the HapMap genotypes (presence or absence of a particular allele) at each locus. $\chi^2$ were calculated for the 2 possible mHag alleles at each locus and the larger value was adopted for each SNP. While different test statistics may be used showing different performance, the $\chi^2$ statistic is most convenient for the purpose of power estimation as described below. The maximum value of the $\chi^2$ statistics was evaluated against the thresholds empirically calculated from 100 000 random permutations within a given LCL set. The program was written in C++ and will run on a unix clone. It will be freely distributed on request. Computation of the statistics was performed within several seconds on a Macintosh equipped with 2 × quadcore 3.2 GHz Zeon processors (Apple, Cupertino, CA), although 100 000 permutations took several hours on average.

### Evaluation of the power of association tests using HapMap samples

The genotyping data of the Phase II HapMap[14] were obtained from the International HapMap Project website (http://www.hapmap.org/genotypes/latest_ncbi_build35), among which we used the nonredundant data sets (excluding SNPs on the Y chromosome) from 60 CEU (Utah residents with ancestry from northern and western Europe) parents, 60 YRI (Yoruba in Ibadan, Nigeria) parents, and the combined set of 45 JPT (Japanese in Tokyo, Japan) and 45 CHB (Han Chinese in Beijing, China) unrelated people. They contained 3 901 416 (2 624 947 polymorphic), 3 843 537 (295 293 polymorphic), and 3 933 720 (2 516 310 polymorphic) SNPs for CEU, YRI, and JPT + CHB, respectively.

To evaluate the power, we first assumed that the Phase II HapMap SNP set contains the target SNP of the relevant mHag or its complete proxies, and that the immunologic assays can completely discriminate $i$ $mHag^+$ and $j$ $mHag^-$ HapMap LCLs. Under this ideal condition, the test statistic, or $\chi^2$, for these SNPs takes a definite value, $f(i,j) = i+j$, which was compared with the maximum $\chi^2$ value, or its distribution, under the null hypothesis, that is, no SNPs within the Phase II HapMap set should be associated with the mHag locus. Unfortunately, the latter distribution cannot be calculated in an explicit analytical form but needs to be empirically determined based on HapMap data, because Phase II HapMap SNPs are mutually interdependent due to extensive linkage disequilibrium within human populations. For this purpose, we simulated 10 000 case-control panels by randomly choosing $i$ $mHag^+$ and $j$ $mHag^-$ HapMap LCLs for various combinations of $(i,j)$ and calculated the maximum $\chi^2$ values ($\chi^2_{max}$) for each panel to identify those $(i,j)$ combinations, in which $f(i,j)$ exceeds the upper 1 percentile point of the simulated 10 000 maximum values, $g(i,j)^{P=.01}$.

When proxies are not complete (ie, $r^2 < 1$), the expected values will be decayed by the factor of $r^2$, and further reduced due to the probabilities of false positive ($f_P$) and negative ($f_N$) assays, and expressed as $\hat{f}(i,j) = (i + j) \times \hat{r}^2$ through an apparent $r^2$ ($\hat{r}^2$) as provided in formula 1.[1] Under given probabilities of assay errors and maximum LD strength between markers and the mHag allele, we can expect to identify target mHag loci for those $(i,j)$ sets that satisfy $\hat{f}(i,j) > g(i,j)^{P=.01}$.

### Empirical estimation of distributions of $r^2$

The maximum $r^2$ value ($r^2_{max}$) between a given mHag allele and one or more Phase II HapMap SNPs was estimated based on the observed HapMap data set. Each Phase II HapMap SNP was assumed to represent a target mHag allele, and the ($r^2_{max}$) was calculated, taking into account all the Phase II HapMap SNPs less than 500 kb apart from the target SNP.

### Confirmatory genotyping

Genotyping was carried out either by TaqMan MGB technology (Applied Biosystems, Foster City, CA) with primers and probes for HA-1 mHag according to the manufacturer's protocol using an ABI 7900HT with the aid of SDS version 2.2 software (Applied Biosystems) or by direct sequencing of amplified cDNA for the *SLC1A5* gene. cDNA was reverse transcribed from total RNA extracted from LCLs, and polymerase chain reaction (PCR) was conducted with cDNA with the corresponding primers. Amplified DNA samples were sequenced using BigDye Terminator version 3.1 (Applied Biosystems). The presence or absence (deletion) of the *UGT2B17* gene was confirmed by genomic PCR with 2 primer sets for exons 1 and 6 as described previously[18] using DNA isolated from LCLs of interest.

### Epitope mapping

A series of deletion mutant cDNAs were designed and cloned into pcDNA3.1/V5-His TOPO plasmid (Invitrogen, Carlsbad, CA). Thereafter, 293T cells that had been transduced with restricting HLA class I cDNA for individual CTL clones were transfected with each of the deletion mutants and cocultured with the CTL clone overnight to induce interferon (IFN)-γ release, which was then evaluated by enzyme-linked immunosorbent assay (ELISA) as previously described.[9]

For *SLC1A5*, expression plasmids encoding full-length cDNA and the exon 1 of recipient and donor origin were first constructed because only the SNP in the exon 1 was found to be concordant with susceptibility to CTL-3B6. Next, amino (N)- and (carboxyl) C-terminus–truncated mini-genes encoding polypeptides around the polymorphic amino acid defined by the SNP were amplified by PCR from *SLC1A5* exon 1 cDNA as template and cloned into the above plasmid. The constructs all encoded a Kozak

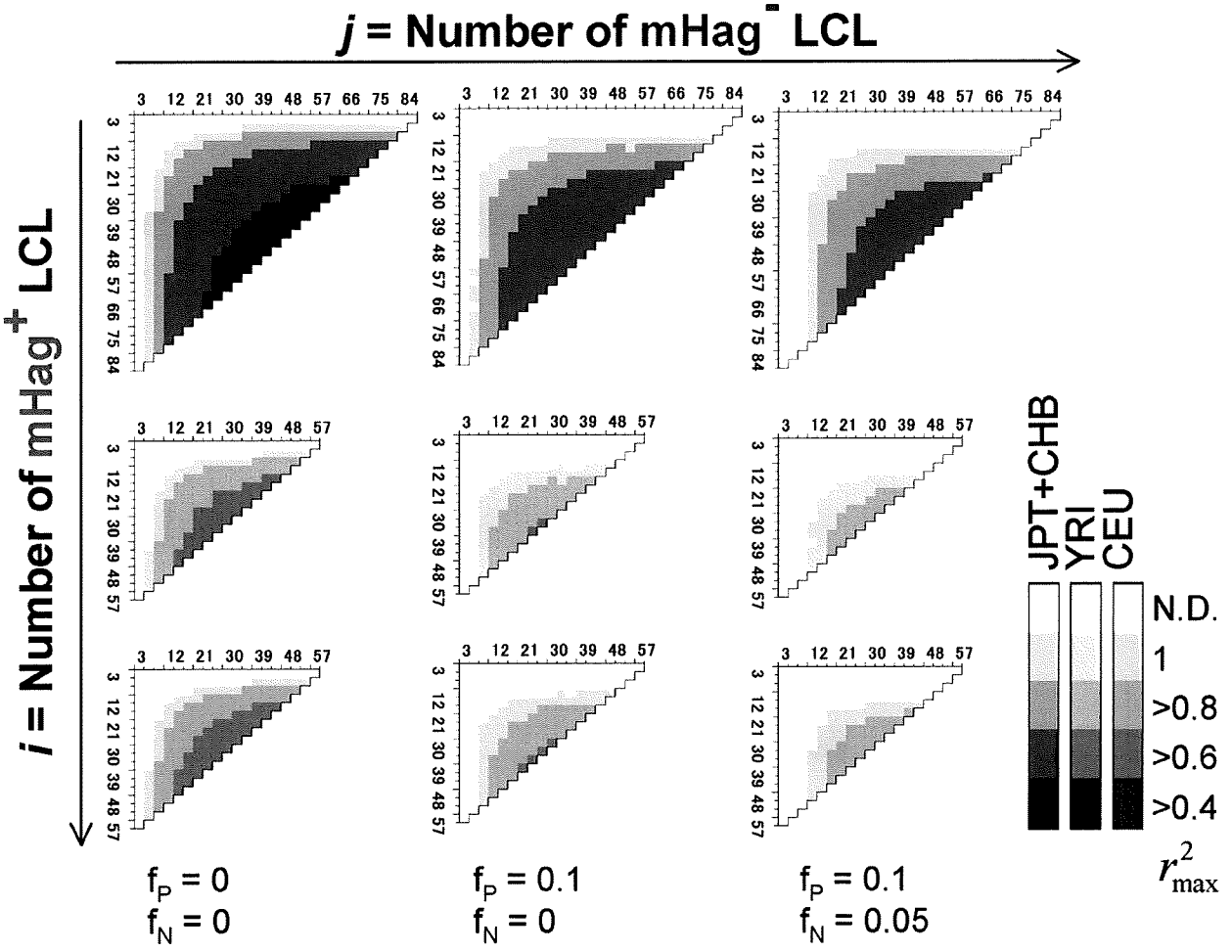


**Figure 1. Numbers of positive and negative LCLs required for successful mHag mapping.** The target locus was assumed to be uniquely identified, if the expected $\chi^2$ value for the target SNP ($\tilde{\chi}(i,j)$, see Document S1) exceeded the upper 1 percentile point of the maximum $\chi^2$ values in 10 000 simulated case-control panels ($g(i,j)^{P=.01}$). Combinations of the numbers of mHag$^+$ (vertical coordinates) and mHag$^-$ (horizontal coordinates) samples satisfying the above condition are shown in color gradients corresponding to different max $r^2$ values between the target SNP and one or more nearby Phase II HapMap SNPs ($r^2_{max}$), ranging from 0.4 to 1.0. Calculations were made for 3 HapMap population panels, CHB + JPT (top), YRI (middle), and CEU (bottom) and for different false positive and negative rates, $f_P = f_N = 0$ (left), $f_P = 0.1, f_N \cong 0$ (middle), and $f_P = 0.1, f_N = 0.05$ (right), considering the very low false negative assays for CRAs.

sequence and initiator methionine (CCACC-ATG) and for C-terminus deletions a stop codon (TAG).

For *UGT2B17*, a series of C-terminus deletion mutants with approximately 200 bp spacing was first constructed as above. For further mapping, N-terminus deletion mutants were added to the region that was deduced to be potentially encoding the CTL-1B2 epitope. For prediction of a CTL epitope, the HLA Peptide Binding Predictions algorithm on the BioInformatics & Molecular Analysis Section (BIMAS) website (http://www.bimas.cit.nih.gov/molbio/hla_bind/)[19] was used because HLA-A*0206 has a similar binding motif to that of A*0201.

### Epitope reconstitution assay

The candidate mHag epitopes and allelic counterpart peptides (in case of SLC1A5) were synthesized by standard Fmoc chemistry. $^{51}$Cr-labeled mHag$^-$ donor LCL were incubated with graded concentrations of the peptides and then used as targets in standard CRAs.

## Results and discussion

### Statistical approach and estimation of potential overfitting

We reasoned that the mHag locus recognized by a given CTL clone could be defined by grouping LCLs from a HapMap panel into mHag$^+$ and mHag$^-$ subpanels according to their susceptibility to lysis by the CTL clone and then performing an association scan using the highly qualified HapMap data set containing more than 3 000 000 SNP markers. The relevant genetic trait here is expected to show near-complete penetrance, and the major concern with this approach arises from the risk of overfitting observed phenotypes to one or more incidental SNPs with this large number of HapMap SNPs under the relatively limited size of freedom due to small numbers of independent HapMap samples (90 for JPT + CHB and 60 for CEU and YRI, when not including their offspring).[13]

To address this problem, we first estimated the maximum sizes of the test statistics (here, $\chi^2$ values) under the null hypothesis (ie, no associated SNPs within the HapMap set) by simulating 10 000 case-control HapMap panels under different experimental conditions, and compared them with the expected size of test statistic values from the marker SNPs associated with the target SNP, assuming different linkage disequilibrium (LD), or $r^2$ values in between. As shown in Figure 1, the possibility of overfitting became progressively reduced as the number of LCLs increased, which would allow for identification of the target locus in a broad range of $r^2$ values, except for those mHags having very low minor allele frequencies (MAF) below

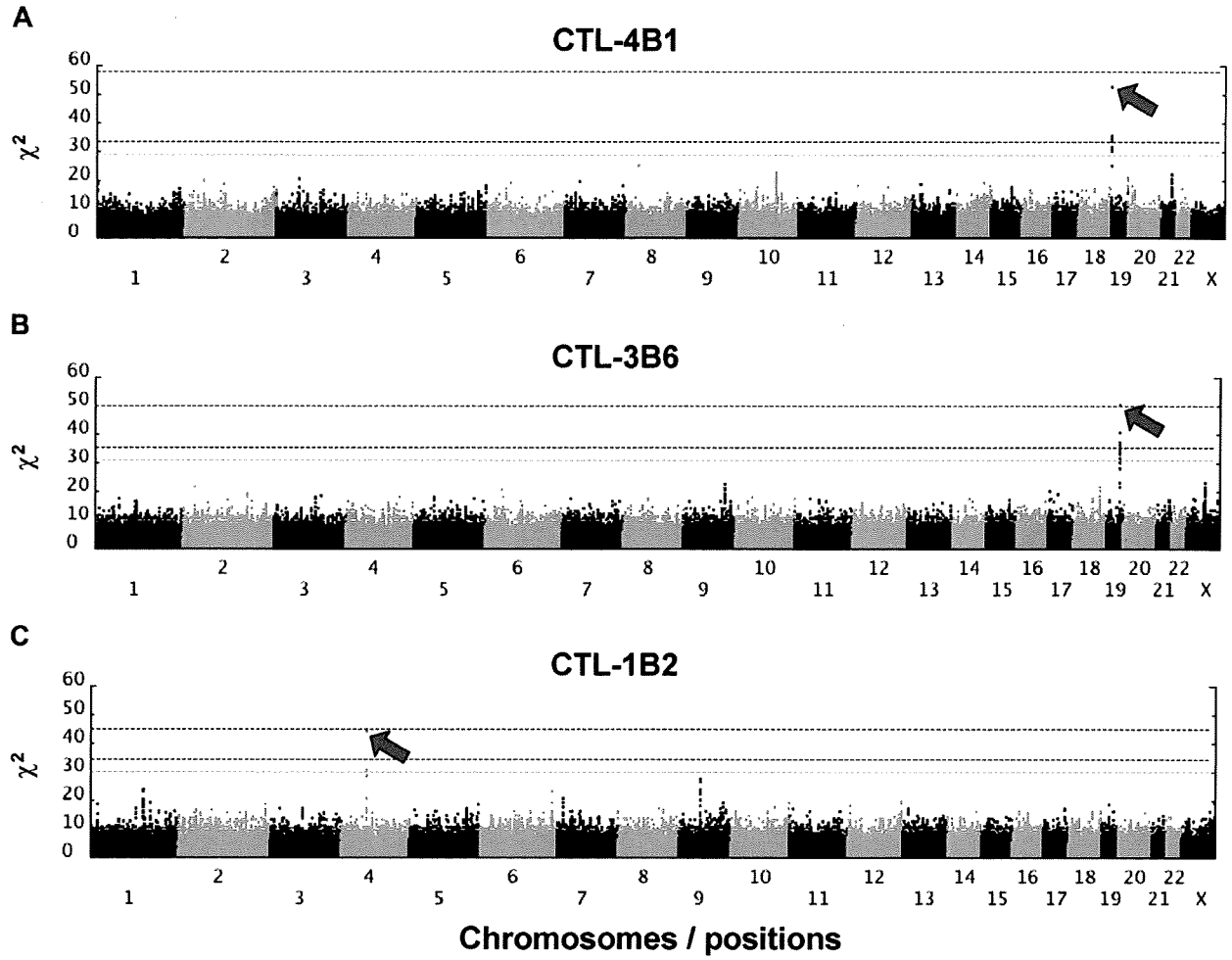


**Figure 2. Genome-wide scanning to identify chromosome location of mHag.** $\chi^2$ values were plotted against positions on each chromosome for each of 3 mHags recognized by CTL-4B1 (A), CTL-3B6 (B), and CTL-1B2 (C). Chromosomes are displayed in alternating colors. Threshold $\chi^2$ values corresponding to the genome-wide $P = 10^{-3}$ (dark blue) and $10^{-2}$ (light blue), as empirically determined from 100 000 random permutations, are indicated by broken lines, while the theoretically possible maximum values are shown with red broken lines. The highest $\chi^2$ value in each experiment is indicated by a red arrow.

approximately 0.05. According to our estimation using the Phase II HapMap data (see "Methods"), the majority (> 90%) of common target SNPs (MAF > ~ 0.05) could be captured by one or more HapMap SNPs with more than 0.8 of $r^2$ (Figure S1, available on the *Blood* website; see the Supplemental Materials link at the top of the online article), ensuring a high probability of detecting an association (Figure 1 left panels). The simulation of pseudo-Phase II sets generated from the ENCODE regions provided a similar estimation.[13] False positive and negative immunophenotyping results could also complicate the detection, reducing the expected test statistics through the "apparent" $r^2$ values ($\hat{r}^2$), as defined by

$$\hat{r}^2 = r^2 \times \frac{(1 - f_P - f_N)^2}{(1 - f_P + f_N q)(1 - f_N + f_P/q)} \quad (1)$$

where $f_P$, $f_N$, and $q$ represent false typing probabilities with positive and negative LCL panels, and the ratio of the positive to the negative LCL number, respectively. However, the high precision of cytotoxicity assays ($f_P \sim < 0.1$, $f_N \sim = 0$) limits this drawback from the second term to within acceptable levels and allows for sensitive mHag locus mapping with practical sample sizes (Figure 1 middle and right panels), suggesting the robustness of our novel approach.

### Evaluation of the detection power for known mHags

Based on these considerations, we then assessed whether this approach could be used to correctly pinpoint known mHag loci (Table S1). Because the relevant mHag alleles are common SNPs and directly genotyped in the Phase II HapMap set, or if not, located within a well-defined LD block recognized in this set (Figure S2), their loci would be expected to be uniquely determined with an acceptable number of samples, as predicted from Figure 1. To test this experimentally, we first mapped the locus for HA-$1^H$ mHag[7] by evaluating recognition of the HLA-A*0206–transduced HapMap cell panel with HLA-A*0206–restricted CTL-4B1.[20] After screening 58 well-growing LCLs from the JPT + CHB panel with CRAs using CTL-4B1 (Figure S3A; Tables S2,S3), we obtained 37 $mHag^+$ and 21 $mHag^-$ LCLs, which were tested for association at 3 933 720 SNP loci. The SNP (rs1801284) encoding the mHag is located within a HapMap LD block on chromosome 19q13.3, but is not directly genotyped within this data set. The genome-wide scan clearly indicated a unique association with the HA-$1^H$ locus within the *HMHA1* gene, showing a peak $\chi^2$ statistic of 52.8 (not reached in 100 000 permutations) at rs10421359 (Figures 2A,3A; Tables S2,S3).

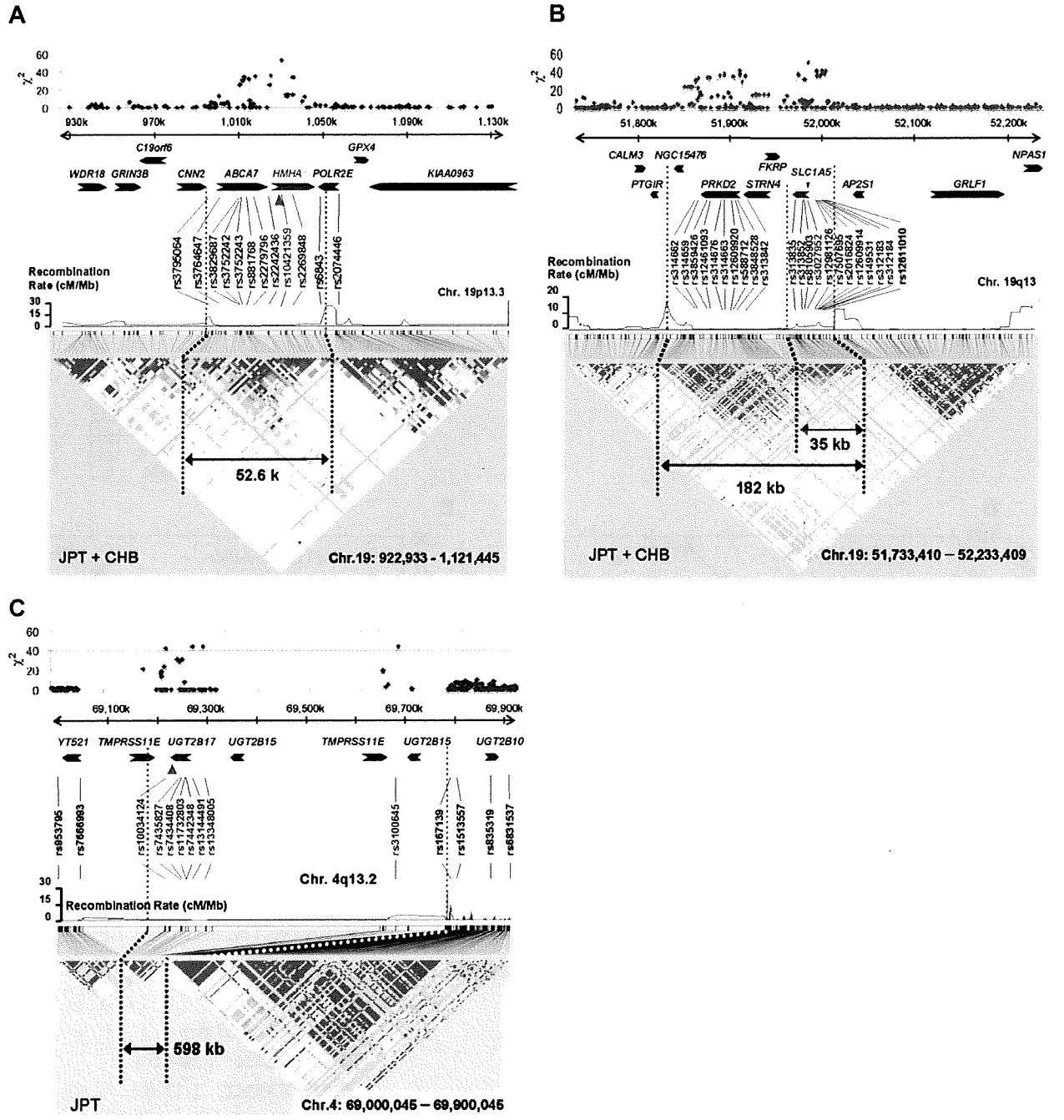


**Figure 3. Regions of mHag loci identified by HapMap scanning.** LD structures around the SNPs showing peak statistical values (in JPT + CHB) are presented for each mHag locus identified with (A) CTL-4B1, (B) CTL-3B6, and (C) CTL-1B2. Regional $\chi^2$ plots are also provided on the top of each panel. LD plots in pairwise D's with recombination rates along the segment were drawn with HaploView software version 4.0 (http://www.broad.mit.edu/mpg/haploview/). The size and location of each LD block containing a mHag locus are indicated within the panels. Significant SNPs (blue letters), as well as other representative SNPs, are shown in relation to known genes. The positions of the SNPs showing the highest statistic values (red letters) are indicated by red arrowheads.

### Identification of novel mHags

We next applied this method to mapping novel mHags recognized by CTL clone 3B6, which is HLA-B*4002–restricted; and CTL clone 1B2, which is HLA-A*0206–restricted. Both clones had been isolated from peripheral blood samples of post-HSCT different patients. In preliminary CRAs with the JPT + CHB panel, allele frequencies of target mHags for CTL-3B6 and CTL-1B2 in this panel were estimated as approximately 25% and approximately 45%, respectively (data not shown). After screening 72 JPT + CHB LCLs with CTL-3B6, 36 mHag$^+$ and 14 mHag$^-$ LCLs were obtained, leaving 22 LCLs undetermined based on empirically determined thresholds ($> 51\%$ for mHag + LCLs and $< 11\%$ for mHag-LCLs; Figure S3B, Tables S2,S4). As shown in Figure 2B, the $\chi^2$ statistics calculated from the immunophenotyping data produced discrete peaks in the LCL sets. The peak in chromosome 19q13.3 for the CTL-3B6 set showed the theoretically maximum $\chi^2$ value of 50 (not reached in 100 000 permutations) at rs3027952, which was mapped within a small LD block of

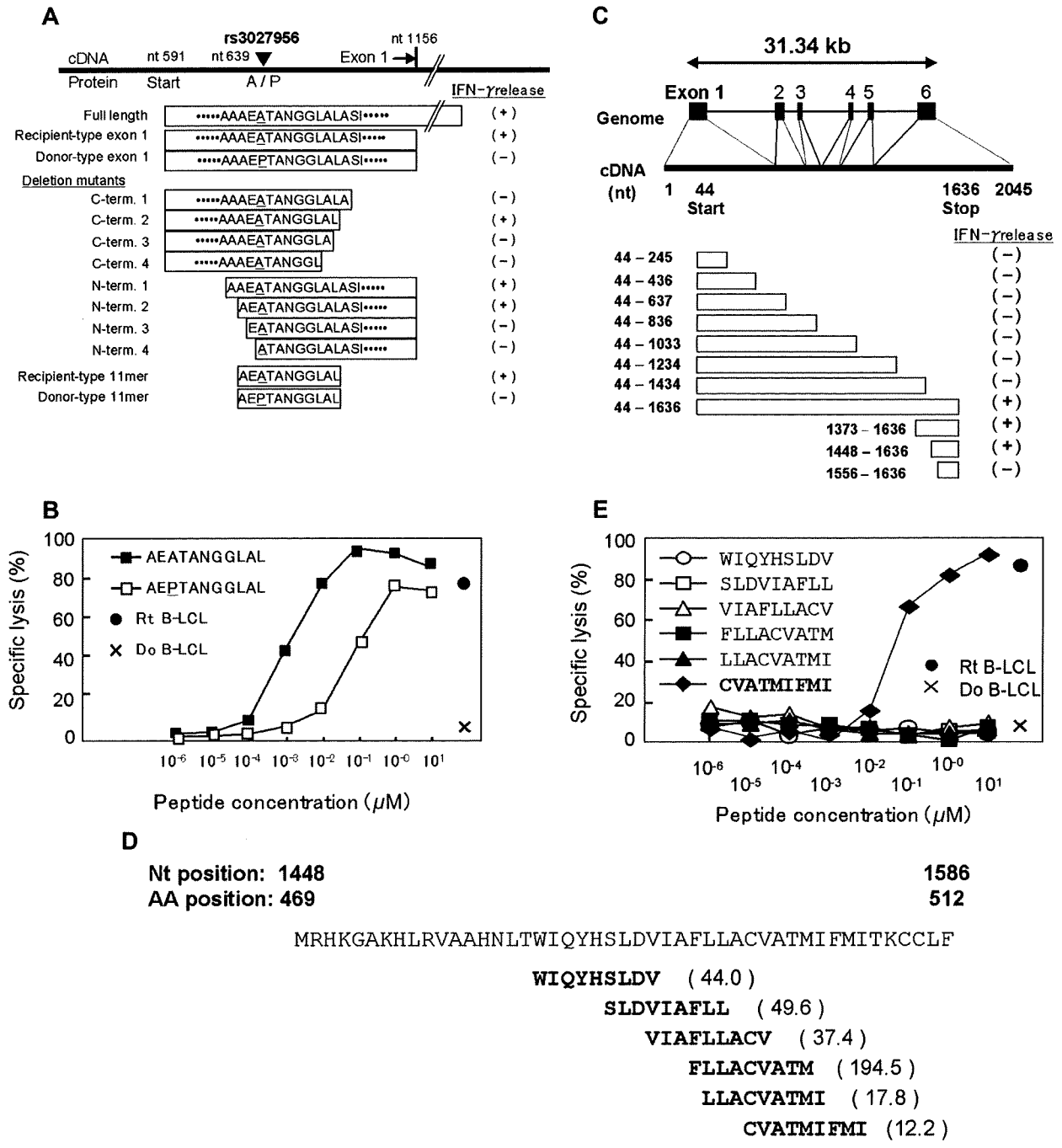


**Figure 4. Epitope mapping.** (A) Determination of the *SLC1A5* epitope by deletion mapping. Plasmids encoding recipient full-length *SLC1A5*, exon 1 of recipient and donor, exon 1 with various N- and C-terminus deletions around the amino acid encoded by SNP rs51983014, and minigenes encoding AEATANGGLAL and its allelic counterpart AEPTANGGLAL were constructed and transfected into HLA-B*4002–transduced 293T cells. Interferon (IFN)-γ was assessed by ELISA (right column) after coculture of CTL-3B1 with 293T transfectants. (B) Epitope reconstitution assay with synthetic undecameric peptides, AEATANGGLAL and AEPTANGGLAL. (C) Structure of the *UGT2B17* gene and screening of *UGT2B17* cDNA and deletion mutants. HLA-A*0206–transduced 293T cells were transfected with each plasmid and cocultured with CTL-2B1. IFN-γ production from CTL-1B2 (right column) indicated that the epitope was likely encoded by nucleotides 1448-1586, including 30 nucleotides from position 1566 that could potentially encode part of the epitope. (D) Epitope prediction using the HLA Peptide Binding Predictions algorithm.[19] Because HLA-A*0201 and -A*0206 have similar peptide binding motifs,[30] the algorithm for HLA-A*0201 was used to predict candidate epitopes recognized by CTL-1B2. Values in parentheses indicate the predicted half-time of dissociation. (E) Epitope reconstitution assays with graded concentrations of synthetic nonameric peptides shown in panel D.

approximately 182 kb, or more narrowly within its 35 kb sub-block containing a single gene, *SLC1A5*, as a candidate mHag gene (Figure 3B). In fact, when expressed in 293T cells with HLA-B*4002 transgene, recipient-derived, but not donor-derived, *SLC1A5* cDNA was able to stimulate IFN-γ secretion from CTL-3B6 (Figure 4A), indicating that *SLC1A5* actually encodes the target mHag recognized by CTL-3B6. Conventional epitope mapping using a series of deletion mutants of *SLC1A5* cDNA finally identified an undecameric peptide, AEATANGGLAL, as the minimal epitope (Figure 4A). The donor-type AEPTANGGLAL induced IFN-γ with a 2-log lower efficiency, suggesting that AEPTANGGLAL may not be transported efficiently into the ER

because endogenous expression of a minigene encoding AEPTANGGLAL was not recognized by CTL-3B1 (Figure 4B). Unfortunately, although the peak statistic value showed the theoretically maximum value for this data set, it did not conform to the relevant SNP for this mHag (rs3027956) due to high genotyping errors of the HapMap data at this particular SNP. However, the result of our resequencing showed complete concordance with the presence of the rs3027956 SNP and recognition in the cytotoxicity assay (Table S4).

Similarly, 13 $mHag^+$ and 32 $mHag^-$ LCLs were identified from the screening of 45 JPT LCLs from the same panel using CTL-1B2 (Figure S3C; Tables S2,S5). The $\chi^2$ statistics calculated from the immunophenotyping data produced bimodal discrete peaks with this LCL set. The target locus for the mHag recognized by CTL-1B2 was identified at a peak (max $\chi^2 = 44$, not reached in 100 000 permutations) within a 598-kb block on chromosome 4q13.1, coinciding with the locus for a previously reported mHag, *UGT2B17*[18] (Figures 2C, 3C). In fact, our epitope mapping using *UGT2B17* cDNA deletion mutants (Figure 4C), prediction of candidate epitopes by HLA-binding algorithms[19] (Figure 4D) and epitope reconstitution assays (Figure 4E), successfully identified a novel nonameric peptide, CVATMIFMI. Of particular note, this mHag was not defined by a SNP but by a CNV (ie, a null allele[18]) that is in complete LD with the SNPs showing the maximum $\chi^2$ value (Table S5). Transplanted T cells from donors lacking both *UGT2B17* alleles are sensitized in recipients possessing at least 1 copy of this gene.[18] Although LD between SNPs and CNVs has been reported to be less prominent,[21] this is an example where a CNV trait could be captured by a SNP-based genome-wide association study.

The recent generation of the HapMap has had a profound impact on human genetics.[13,15] In the field of medical genetics, the HapMap is a central resource for the development of theories and methods that have made well-powered, genome-wide association studies of common human diseases a reality.[22-28] The HapMap samples provide not only an invaluable reference for genetic variations within human populations, but highly qualified genotypes that enable gene-wide scanning. Here, we have demonstrated how effectively HapMap resources can be used for genetic mapping of clinically relevant human traits. No imputations and tagging strategies are required[25,28] and the potential loss of statistical power due to very limited sample sizes is circumvented by accurate immunologic detection of the traits.

Using publicly available HapMap resources, high-throughput identification of mHag genes is possible without highly specialized equipment or expensive microarrays. Except for clinically irrelevant mHags with very low allele frequencies (eg, MAF < 5%), the target of a given CTL can be sensitively mapped within a mean LD block size, typically containing just a few candidate genes. The methodology described here will facilitate construction of a large panel of human mHags including those presented by MHC class II molecules, and promote our understanding of human allo-immunity and development of targeted allo-immune therapies for hematologic malignancies.[1,2] The HapMap scan approach may be useful for exploring other genetic traits or molecular targets (eg, differential responses to some stress or drugs), if they can be discriminated accurately through appropriate biologic assays. In this context, the recent report that we may reprogram the fate of terminally differentiated human cells[29] is encouraging, indicating possible exploration of genotypes that are relevant to cell types other than immortalized B cells.

## Acknowledgments

We thank Drs P. Martin and W. Ho for critically reading the manuscript; and Ms Keiko Nishida, Dr Ayako Demachi-Okamura, Dr Yukiko Watanabe, Ms Hiromi Tamaki, and the staff members of the transplant centers for their generous cooperation and technical expertise.

This study was supported in part by a grant for Scientific Research on Priority Areas (B01; no.17016089) from the Ministry of Education, Culture, Science, Sports, and Technology, Japan; grants for Research on the Human Genome, Tissue Engineering Food Biotechnology and the Second and Third Team Comprehensive 10-year Strategy for Cancer Control (no. 26) from the Ministry of Health, Labor, and Welfare, Japan; and a grant-in-aid from Core Research for Evolutional Science and Technology (CREST) of Japan.

## Authorship

Contribution: M.K. performed most of immunologic experiments and analyzed data and wrote the manuscript; Y.N. performed the majority of genetic analyses and analyzed the data; H.T., T.K., M.Y., S.M. and K.Tsujimura performed research; K.Taura contributed to the computational simulation; Y.I., Taro T., K.M., Y.K. and Y.M. collected clinical data and specimens; T.I., H.T., S.R.R., Toshitada T. and K.K. contributed to data analysis and interpretation, and writing of the article; and Y.A. and S.O. supervised the entire project, designed and coordinated most of the experiments in this study, and contributed to manuscript preparation.

Conflict-of-interest disclosure: The authors declare no competing financial interests.

Correspondence: Seishi Ogawa, MD, PhD, Department of Hematology and Oncology, Department of Regeneration Medicine for Hematopoiesis, The 21st Century COE Program, Graduate School of Medicine, University of Tokyo, 7-3-1, Hongo, Bunkyo-ku, Tokyo 113-8655, Japan; e-mail: sogawa-tky@umin.ac.jp; or Yoshiki Akatsuka, MD, PhD, Division of Immunology, Aichi Cancer Center Research Institute, 1-1 Kanokoden, Chikusa-ku, Nagoya 464-8681, Japan; e-mail: yakatsuk@aichi-cc.jp.

## References

1. Bleakley M, Riddell SR. Molecules and mechanisms of the graft-versus-leukaemia effect. Nat Rev Cancer. 2004;4:371-380.
2. Spierings E, Goulmy E. Expanding the immunotherapeutic potential of minor histocompatibility antigens. J Clin Invest. 2005;115:3397-3400.
3. de Rijke B, van Horssen-Zoetbrood A, Beekman JM, et al. A frameshift polymorphism in P2X5 elicits an allogeneic cytotoxic T lymphocyte response associated with remission of chronic myeloid leukemia. J Clin Invest. 2005;115:3506-3516.
4. Marijt WA, Heemskerk MH, Kloosterboer FM, et al. Hematopoiesis-restricted minor histocompatibility antigens HA-1- or HA-2-specific T cells can induce complete remissions of relapsed leukemia. Proc Natl Acad Sci U S A. 2003;100:2742-2747.
5. Spierings E, Hendriks M, Absi L, et al. Phenotype frequencies of autosomal minor histocompatibility antigens display significant differences among populations. PLoS Genet. 2007;3:e103.
6. Brickner AG, Warren EH, Caldwell JA, et al. The immunogenicity of a new human minor histocompatibility antigen results from differential antigen processing. J Exp Med. 2001;193:195-206.
7. den Haan JM, Meadows LM, Wang W, et al. The minor histocompatibility antigen HA-1: a diallelic gene with a single amino acid polymorphism. Science. 1998;279:1054-1057.

8. Dolstra H, Fredrix H, Maas F, et al. A human minor histocompatibility antigen specific for B cell acute lymphoblastic leukemia. J Exp Med. 1999; 189:301-308.
9. Kawase T, Akatsuka Y, Torikai H, et al. Alternative splicing due to an intronic SNP in HMSD generates a novel minor histocompatibility antigen. Blood. 2007;110:1055-1063.
10. Akatsuka Y, Nishida T, Kondo E, et al. Identification of a polymorphic gene, BCL2A1, encoding two novel hematopoietic lineage-specific minor histocompatibility antigens. J Exp Med. 2003;197: 1489-1500.
11. Kawase T, Nanya Y, Torikai H, et al. Identification of human minor histocompatibility antigens based on genetic association with highly parallel genotyping of pooled DNA. Blood. 2008;111:3286-3294.
12. Risch N, Merikangas K. The future of genetic studies of complex human diseases. Science. 1996;273:1516-1517.
13. The International HapMap Consortium. The International HapMap Project. Nature. 2003;426:789-796.
14. The International HapMap Consortium. A second generation human haplotype map of over 3.1 million SNPs. Nature. 2007;449:851-861.
15. The International HapMap Consortium. A haplotype map of the human genome. Nature. 2005; 437:1299-1320.
16. Akatsuka Y, Goldberg TA, Kondo E, et al. Efficient cloning and expression of HLA class I cDNA in human B-lymphoblastoid cell lines. Tissue Antigens. 2002;59:502-511.
17. Riddell SR, Greenberg PD. The use of anti-CD3 and anti-CD28 monoclonal antibodies to clone and expand human antigen-specific T cells. J Immunol Methods. 1990;128:189-201.
18. Murata M, Warren EH, Riddell SR. A human minor histocompatibility antigen resulting from differential expression due to a gene deletion. J Exp Med. 2003;197:1279-1289.
19. Parker KC, Bednarek MA, Coligan JE. Scheme for ranking potential HLA-A2 binding peptides based on independent binding of individual peptide side-chains. J Immunol. 1994;152:163-175.
20. Torikai H, Akatsuka Y, Miyauchi H, et al. The HLA-A*0201-restricted minor histocompatibility antigen HA-1H peptide can also be presented by another HLA-A2 subtype, A*0206. Bone Marrow Transplant. 2007;40:165-174.
21. Redon R, Ishikawa S, Fitch KR, et al. Global variation in copy number in the human genome. Nature. 2006;444:444-454.
22. Barrett JC, Cardon LR. Evaluating coverage of genome-wide association studies. Nat Genet. 2006;38:659-662.
23. Nannya Y, Taura K, Kurokawa M, Chiba S, Ogawa S. Evaluation of genome-wide power of genetic association studies based on empirical data from the HapMap project. Hum Mol Genet. 2007;16:2494-2505.
24. Pe'er I, de Bakker PI, Maller J, Yelensky R, Altshuler D, Daly MJ. Evaluating and improving power in whole-genome association studies using fixed marker sets. Nat Genet. 2006;38:663-667.
25. Marchini J, Howie B, Myers S, McVean G, Donnelly P. A new multipoint method for genome-wide association studies by imputation of genotypes. Nat Genet. 2007;39:906-913.
26. Altshuler D, Daly M. Guilt beyond a reasonable doubt. Nat Genet. 2007;39:813-815.
27. Bowcock AM. Genomics: guilt by association. Nature. 2007;447:645-646.
28. de Bakker PI, Burtt NP, Graham RR, et al. Transferability of tag SNPs in genetic association studies in multiple populations. Nat Genet. 2006;38: 1298-1303.
29. Takahashi K, Tanabe K, Ohnuki M, et al. Induction of pluripotent stem cells from adult human fibroblasts by defined factors. Cell. 2007;131: 861-872.
30. Sudo T, Kamikawaji N, Kimura A, et al. Differences in MHC class I self peptide repertoires among HLA-A2 subtypes. J Immunol. 1995;155: 4749-4756.

Int J Hematol (2008) 87:467–473
DOI 10.1007/s12185-008-0076-5

ORIGINAL ARTICLE

# Aberrant expression of BCL2A1-restricted minor histocompatibility antigens in melanoma cells: application for allogeneic transplantation

**Hiroki Torikai · Yoshiki Akatsuka · Yasushi Yatabe · Yasuo Morishima · Yoshihisa Kodera · Kiyotaka Kuzushima · Toshitada Takahashi**

Received: 30 November 2007 / Revised: 7 March 2008 / Accepted: 14 March 2008 / Published online: 15 April 2008


**Abstract** It has been shown that allogeneic hematopoietic stem cell transplantation (HSCT) can be one of the therapeutic options for patients with metastatic solid tumors, such as renal cancer. However, the development of relatively severe GVHD seems to be necessary to achieve tumor regression in the current setting. Thus, it is crucial to identify minor histocompatibility antigens (mHags) only expressed in tumor cells but not GVHD target organs. In this study, we examined whether three mHags: ACC-1 and ACC-2 encoded by *BCL2A1*, and HA-1 encoded by *HMHA1*, could serve as such targets for melanoma. Real-time PCR and immunohistochemical analysis revealed that the expression of both *BCL2A1*and *HMHA1* in melanoma cell lines and primary melanoma cells was comparable to that of hematopoietic cells. Indeed, melanoma cell lines were efficiently lysed by cytotoxic T lymphocytes specific for ACC-1, ACC-2, and HA-1. Our data suggest that targeting mHags encoded not only by *HMHA1*, whose aberrant expression in solid tumors has been reported, but also *BCL2A1* may bring about beneficial selective graft-versus-tumor effects in a population of melanoma patients for whom these mHags are applicable.

**Keywords** Minor histocompatibility antigen · Allogeneic hematopoietic stem cell transplantation · Melanoma

H. Torikai · Y. Akatsuka (✉) · K. Kuzushima · T. Takahashi
Division of Immunology, Aichi Cancer Center Research Institute, 1-1 Kanokoden, Chikusa-ku, Nagoya 464-8681, Japan
e-mail: yakatsuk@aichi-cc.jp

Y. Yatabe
Department of Pathology and Molecular Diagnostics, Aichi Cancer Center Central Hospital, Nagoya, Japan

Y. Morishima
Department of Hematology and Cell Therapy, Aichi Cancer Center Central Hospital, Nagoya, Japan

Y. Kodera
Department of Hematology, Japanese Red Cross Nagoya First Hospital, Nagoya, Japan

## 1 Introduction

Allogeneic hematopoietic stem cell transplantation (HSCT) can cure hematopoietic malignancies. The success of donor leukocyte infusion or a non-myeloablative conditioning regimen demonstrated that the therapeutic effects of allogeneic HSCT mostly rely on the allogeneic immune responses. In an HLA-matched setting, allogeneic immune responses are mediated by donor-derived cytotoxic T lymphocytes (CTLs) against minor histocompatibility antigens (mHags). Ubiquitously expressed mHags are responsible for both life-threatening graft-versus-host disease (GVHD) and the graft-versus-leukemia (GVL) effect, whereas hematopoietic cell-restricted mHags, such as HA-1 [1] or ACC-6 [2], may be optimal target antigens which can potentially separate the GVL effect from GVHD development [3].

In some solid tumors, such as melanoma or renal cell carcinoma, there has been accumulating evidence that immunological manipulation, e.g., IL-2 [4, 5] or interferon treatment [6], can lead to clinical responses in some patients with refractory disease, although responses have been limited. Since the late 1990s, it has been reported that nonmyeloablative allogeneic HSCT leads to apparent tumor regression in these immunogenic solid tumors [7, 8]. However, the development of relatively severe GVHD seems to be necessary to achieve tumor regression in the

current setting. Thus, it is crucial to identify antigens that may serve as therapeutic targets for post-transplant vaccination or adoptive T-cell therapy to selectively augment the graft-versus-tumor (GVT) effects following allogeneic HSCT with modification to reduce fatal GVHD. Recently, we and others showed that the hematopoietic cell-restricted mHag HA-$1^H$, encoded by *HMHA1*, can be one of the potential targets for the GVT effect due to its aberrant expression in some solid tumors [9–11]. In addition, *ECGF1*-encoded mHag has been shown to be expressed in some solid tumors [12]. Thus, we sought to examine whether other mHags we had identified previously could also be expressed in any solid tumors and serve as potential targets for GVT effects.

The ACC-1 and ACC-2 mHags encoded by *BCL2A1* have been shown as hematopoietic cell lineage-restricted mHags [13]. Amino acid substitutions, $^{19}$Cysteine→Tyrosine, and $^{82}$Glycine→Aspartic acid, of BCL2A1 lead to donor-derived HLA-A*2402 and HLA-B*4403/4402-restricted $CD8^+$ CTL responses against the recipient's hematopoietic cells [13]. In this study, we demonstrate that *BCL2A1* is also highly expressed in melanoma cells and that they are effectively lysed by cognate CTLs. Although it has been reported that allogeneic HSCT was not promising against advanced melanoma in a small cohort of patients [14], our findings imply that targeting *BCL2A1*-encoded mHags may bring about beneficial GVT effects in a fraction of melanoma patients for whom these mHags are applicable.

## 2 Materials and methods

### 2.1 Cell lines and cell culture

$CD8^+$CTL clones recognizing $ACC1^Y$ (1B3-CTL) and ACC-$2^D$ (3B5-CTL) were generated from post-HSCT recipients peripheral blood mononuclear cells (PBMCs) and HA-$1^H$ (EH6-CTL) were from healthy volunteer's PBMCs, as previously described [11, 13]. These CTL clones were expanded using allogeneic PBMCs and Epstein Barr virus-transformed B cell lines (B-LCLs) as feeder cells and frozen until use.

Table 1 indicates the melanoma cell lines used in this study, kindly provided by Dr. Kawakami (Keio University, Tokyo, Japan). Their genotypes for the HLA class I and mHag allele were typed at the HLA Laboratory (Kyoto, Japan). All melanoma cell lines were cultured in Iscove modified Dulbecco medium (Invitrogen, Carlsbad, CA, USA) supplemented with 10% fetal calf serum (FCS), 2 mM L-glutamine, and penicillin/streptomycin. B-LCLs established by infecting PBMCs with B95-8 (ATCC, Rockville, MD, USA) supernatant and HLA class I-deficient mutant 721.221 B-LCL were cultured in RPMI1640 supplemented with 10% FCS, 2 mM L-glutamine, 1 mM sodium pyruvate, and penicillin/streptomycin. Primary melanocytes, NHE-Ma(L) and HEMa-LP, were purchased from KURABO (Osaka, Japan) and cultured in specified medium according to the manufacturer's protocol. All blood and tissue samples were collected after obtaining written informed consent, and the study was approved by the Institutional Review Board of Aichi Cancer Center.

**Table 1** HLA and mHags typing of melanoma cell lines

| Cell line | HLA | | mHag [a] | | |
|---|---|---|---|---|---|
| | A loci | B loci | ACC-1 | ACC-2 | HA-1 |
| 888Mel | 0101/2402 | 5201/5501 | Y/C | D/G | R/R |
| HT144 | 0101/2402 | 1501/5701 | Y/C | D/G | R/R |
| G361 | 2301/2601 | 3801/4403 | Y/C | D/G | R/R |
| WM266 | 0201/2902 | 1302/4403 | C/C | G/G | H/R |
| C32Mel | 0201/2501 | 1801/4402 | C/C | G/G | H/H |
| HS294T | 0101/2501 | 0702/0801 | C/C | G/G | R/R |

[a] The phenotypes of mHags of individual melanoma cell lines are shown using a single-lettered amino acid code. ACC-1 mHag is considered to be positive when carrying a Y (tyrosine) residue (referred to as $ACC\text{-}1^Y$) at its polymorphic site, while it is negative when carrying a C (cysteine) residue (referred to as $ACC\text{-}1^C$). Similarly, $ACC\text{-}2^D$ carrying D (asparaginic acid) is positive, while $ACC\text{-}2^G$ carry G (glycine) is negative; HA-$1^H$ carrying H (histidine) is positive, while HA-$1^R$ carrying R (arginine) is negative

### 2.2 Messenger RNA expression of BCL2A1 and HMHA1 in melanoma cell lines

Total RNA was extracted using the RNeasy Mini Kit (Qiagen). Messenger RNA was magnetically isolated from total RNA using the μMACS mRNA Isolation kit (Miltenyi Biotec) according to the manufacturer's protocol. Complementary DNA was synthesized in the presence of oligo $(dT)_{15}$ primer (Roche) and M-MLV-reverse transcriptase (Invitrogen) according to the manufacturers' instructions.

PCR amplification and real-time quantification analysis were performed using the TaqMan assay according to the manufacturer's instructions. The following sequences were used as primers with the TaqMan probe to detect the mRNA region of each gene:

BCL2A1-sense: 5′-TGAATAACACAGGAGAATGGATAAGG-3′,
BCL2A1-antisense: 5′-TTCAGGAGAGATAGCATTTCACAGAT-3′,
BCL2A1-probe: 5′-(FAM)-CTGGCTGGATGACTTT-(MGB)-3′
HMHA1-sense: 5′-GAGGGCCTTGAGAAACTTAAGGA-3′

HMHA1-antisense: 5′-CAGCGGGTACTTGGAGATG ATC-3′,
HMHA1-probe; 5′-(FAM)-CTGCGTGTCATGCAT-(MGB)-3′

For an internal control, a primer and probe set for human Glyceraldehyde-3-phosphate dehydrogenase (GAPDH) (Applied Biosystems) was used. PCR was performed in a 1 × TaqMan Universal PCR master mix containing 10 pmol of each sense and antisense primer, and 2 pmol of probe in a total volume of 25 μL in the ABI PRISM 7900HT Sequence Detector System (Applied Biosystems). The temperature profile was: 50°C for 2 min, 95°C for 10 min, and then 95°C for 15 s and 60°C for 1 min for 40 cycles. Relative expressions were calculated by the $_{\Delta\Delta}C_T$ method after validation test described in the manufacturer's brochure (User Bulletin #2; Applied Biosystems 11 December 1997 (updated October 2001).

### 2.3 Immunohistochemical analysis of BCL2A1 expression in primary melanoma

To analyze the BCL2A1 protein expression in primary melanoma cells, we used frozen skin sections obtained from six patients with metastatic melanoma. The expression status was examined immunohistochemically with the standard avidin–biotin–peroxidase complex method using polyclonal antibodies against BCL2A1 [Santa Cruz, A1 (N-20): sc-6066].

### 2.4 Flow cytometric analysis of HLA Class I and BCL2A1 expression in melanoma cell lines

The cell surface HLA-class I expression of melanoma cell lines before and after treatment with interferon-γ (IFN-γ) and TNF-α was evaluated using W6/32 mAb (10 μg/mL) and FITC-conjugated anti-mouse IgG antibodies (Beckman Coulter). For the intracellular staining of BCL2A1 protein, cells were fixed and permeabilized with Cytofix/Cytoperm (BD Biosciences), washed once with PBS, and incubated with 40 μg/mL of goat polyclonal antibodies against BCL2A1 [Santa Cruz, A1 (N-20): sc-6066] for 15 min. After washing, bound antibodies were detected by incubation with FITC-conjugated donkey anti-goat IgG antibody (8 μg/mL, Santa Cruz, CA, USA) for 15 min. Cells were analyzed with a FACS Calibur flow cytometer and CellQuest software (Becton-Dickinson).

### 2.5 Cytotoxicity assay

Target cells were labeled with 0.1 mCi of $^{51}Cr$ for 2 h or overnight at 37°C, and 1 × $10^3$ target cells/well were mixed with CTLs at an E/T ratio indicated in a standard 4-h cytotoxicity assay using 96 well, round-bottomed plates. All assays were performed at least in duplicate. Cells were treated either with IFN-γ (500 U/mL, R&D Systems) or TNF-α (10 ng/mL, Genzyme) for 48 h as indicated. Percent specific lysis was calculated as follows: ((Experimental cpm − Spontaneous cpm) / (Maximum cpm − Spontaneous cpm)) × 100.

## 3 Results

### 3.1 Melanoma cell lines express high levels of BCL2A1 gene

We previously demonstrated that *BCL2A1* is preferentially expressed in hematopoietic lineage cells but not other normal cells. By accessing a gene expression database, GNF (Genomic Institute of the Novartis Research Foundation, http://symatlas.gnf.org/SymAtlas/) [15], we found that *BCL2A1* is highly expressed in melanoma cell lines. Thus, we first tried to confirm the expression levels of *BCL2A1* in melanoma cell lines using real-time PCR. As shown in the lower part of Fig. 1a, most melanoma cell lines expressed the *BCL2A1* transcript at levels as high as B-LCLs, with the exception of the cell line HS294T, which eventually expressed a comparable level of the transcript after cytokine treatment (IFN-γ and TNF-α). Some cell lines also expressed *HMHA1* transcripts, but their levels were relatively low (Fig. 1b).

### 3.2 BCL2A1 expression in primary melanoma specimens

We subsequently tested whether primary melanoma cells expressed BCL2A1 protein. Skin sections from six patients (MM-1 to MM-6) with metastatic melanoma were stained with anti-BCL2A1 antibody (Fig. 2). Three specimens were positive for BCL2A1 (MM-1, 2, 3), while one was negative (MM-4). Another two samples were difficult to evaluate because of marked melanin pigmentation (MM-5, 6). Overall, 3/4 primary metastatic melanoma cells were positive for BCL2A1 protein. Along with the results of real-time PCR analysis, BCL2A1 was strongly and frequently expressed in melanoma cells.

### 3.3 Melanoma cell lines are susceptible to lysis by BCL2A1-specific CTL clones

To determine whether melanoma cell lines can indeed present BCL2A1-derived mHags on their cell surface HLA molecules, and are thus susceptible to lysis by CTLs specific for these mHags, we performed a standard

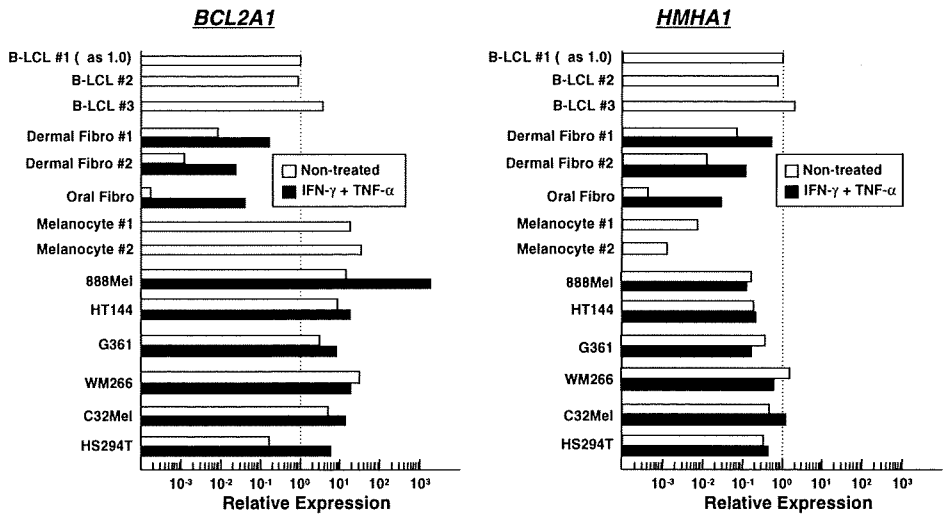


**Fig. 1** Relative expression of *BCL2A1* (*left panel*) and *HMHA1* (*right panel*) in melanoma cell lines. Real-time reverse transcription PCR to quantify the mRNA expression of *BCL2A1* and *HMHA1* was performed using cDNA samples prepared from melanoma cell lines (kind gift from Dr. Kawakami, Keio University, Tokyo) and primary melanocytes, together with EBV-transformed B lymphoblasts (B-LCLs) and fibroblasts (Fibro) from skin and oral mucosa. IFN-$\gamma$ + TNF-$\alpha$ (*solid bars*) denotes 48-h cytokine treatment with 500 U/mL of IFN-$\gamma$ and 10 ng/mL of TNF-$\alpha$. *GAPDH* was used as an internal control. mRNA expression in B-LCLs is set as 1.0

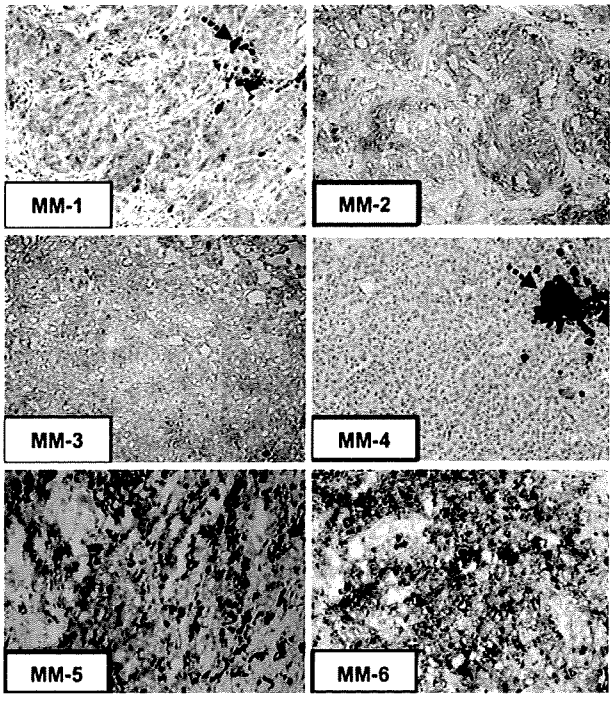


**Fig. 2** Expression of BCL2A1 protein in primary metastatic melanoma (MM) cells. Frozen skin sections from six patients with metastatic melanoma were examined for BCL2A1 expression immunohistochemically by the standard avidin–biotin–peroxidase complex method using polyclonal antibodies against BCL2A1 (Santa Cruz, A1 (N-20): sc-6066). MM-1 to -3 were found to be positive; MM-4 negative; MM-5 and -6 showed marked melanin pigmentation. *Red arrows* in MM-1 and MM-4 indicate melanin spots, showing that the specimens were of melanoma origin

$^{51}$Cr-release assay. As shown in Fig. 3a, melanoma cell lines positive for respective mHags and restriction HLA alleles were lysed effectively by cognate CTL clones: 888Mel and HT144 by 18B3-CTL (HLA-A24-restricted, ACC-1$^{Y}$-specific), and G361 by 3B5-CTL (HLA-B44-restricted, ACC-2$^{D}$-specific). In contrast, HLA-class I-deficient K562 cell lines or melanoma cell lines lacking either the restriction HLA allele or cognate mHag allele that were used as control targets were not lysed at all, indicating that the observed cytotoxicity against melanoma cell lines by these CTL clones was antigen-specific. We also examined the expression of HLA-class I and intracellular BCL2A1 in these cell lines to evaluate the effect of cytokine treatment. All melanoma cell lines tested were positive for HLA-class I and BCL2A1, similarly to B-LCLs, with the one exception of HT144, whose BCL2A1 expression was 1-log lower than that of B-LCLs (Fig. 3B). Cytokine treatment upregulated HLA-class I expression in all melanoma cell lines, with one exception of 888 MEL, which might account for the increased lysis of G361 by 3B5-CTL and WM266 by EH6-CTL, respectively. The lower BCL2A1 expression in HT144 was also upregulated after treatment. However, cytokine treatment did not necessarily result in increased, specific lysis in cell lines other than G361 and WM266. Therefore, another mechanism might also be involved in the susceptibility to lysis of each cell line. In addition, two melanoma cell lines (WM266 and C32Mel) positive for the HLA-A*0201 and HA-1$^{H}$ alleles could be recognized by EH6-CTL despite the relatively low expression of *HMHA1* compared to *BCL2A1*.

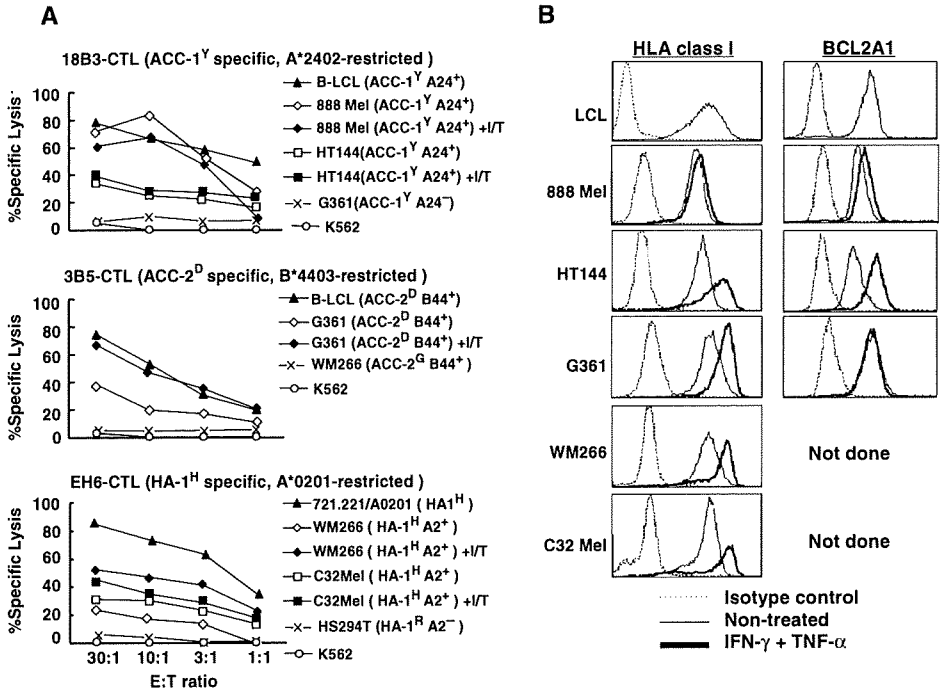


**Fig. 3** Susceptibility of melanoma cell lines to mHag-specific CTL clones and the impact of cytokine treatment. **a** $^{51}$Cr-release assay against melanoma cell lines. Standard 4-h $^{51}$Cr-release assays were performed against various melanoma cell lines at the indicated E/T ratios and at least in duplicate. B-LCLs positive for the restriction HLA allele and mHag allele were used as positive controls for individual CTL clones. The 721.221 cell line comprised HLA-A*0201-transduced B-LCLs positive for the HA-1$^{H}$ allele. Non-specific lysis of the individual CTL clones was examined and verified by testing against NK cell-sensitive K562 or melanoma cell lines that lacked either the cognate mHag or restriction HLA allele. I/T denotes the treatment of indicated cell lines with 500 U/mL of IFN-$\gamma$ and 10 ng/mL of TNF-$\alpha$ for 48 hours prior to assays; **b** HLA class I and BCL2A1 expression of melanoma cell lines. Cell surface expression of HLA class I and intracellular staining of BCL2A1 was evaluated by flow cytometry before and after treatment with the above cytokines

### 3.4 HMHA1 in dermal fibroblasts is also upregulated by inflammatory cytokines

It has been reported that *HMHA1* encoding HA-1 mHag is not detected in normal nonhematopoietic cells such as dermal fibroblasts [9], while *BCL2A1* is upregulated in bone marrow-derived mesenchymal stem cells by inflammatory cytokines [16]. Thus, we examined whether dermal fibroblasts upregulated these mHag genes and became susceptible to cognate CTL clones. We found that the expression of both *BCL2A1* and *HMHA1* is upregulated in the dermal fibroblasts after cytokine treatment (Fig. 1a, b, upper part), indicating that these hematopoietic cell-specific mHags might be induced in a strong inflammatory cytokine milieu such as active GVHD after HSCT. Hematopoietic cell contamination was excluded by real-time PCR or flow cytometric analysis of the expression of CD45 in these fibroblasts (data not shown). Coincident with expression, the HLA-A*0201-restricted HA-1$^{H}$-specific CTL clone, EH6-CTL, and A*2402 restricted ACC-1$^{Y}$ specific CTL clone, 18B3-CTL, could lyse these cytokine-treated mHag-positive dermal fibroblasts, although their level of lysis was relatively lower than that of hematopoietic cells (Fig. 4a, b).

## 4 Discussion

In this study, we demonstrated that HLA-A24-restricted ACC-1$^{Y}$ and HLA-B44-restricted ACC-2$^{D}$ mHAgs, whose expressions were shown to be limited to hematopoietic cells including leukemia cells, were also expressed in melanoma cell lines by real-time PCR and cytotoxicity assays. Melanoma is known as one of the representative immunogenic tumors. Previously, IL-2 administration [4] or the infusion of ex vivo expanded TILs [17] was tested, but resulted in a limited clinical response. In 1990s, many antigens of melanoma origin recognized by autologous T lymphocytes were identified [18], and these antigens were subsequently tested in clinical trials by peptide vaccination or adoptive CTL infusion. To date, peptide vaccination has resulted in a limited or marginal efficacy [19] while adoptive T lymphocyte infusion including Ag-specific CTL clones or TILs, especially after a lymphodepleted conditioning regimen,

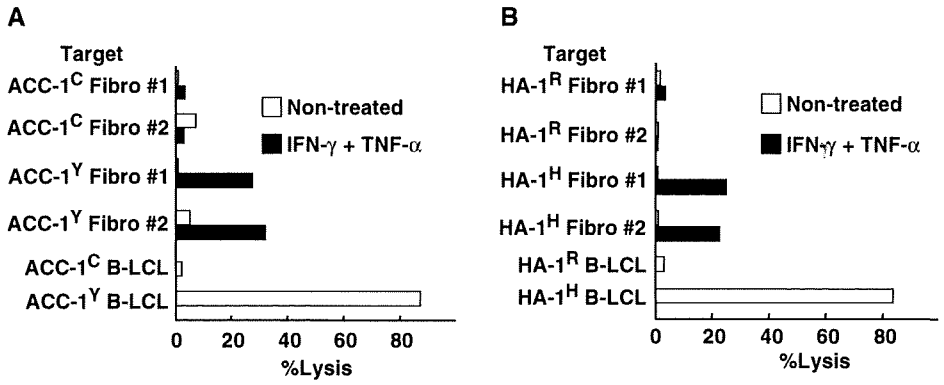


**Fig. 4** Cytotoxicity of mHag-specific CTL clones against dermal fibroblasts. A standard 4-h $^{51}$Cr-release assay was performed, as described above. **a** Cytotoxic activity of the HLA-A*2402-restricted, ACC-1$^{Y}$ mHag-specific 1B3-CTL clone against HLA-A*2402-positive dermal fibroblasts (Fibro) and B-LCLs that were either ACC-1$^{Y}$ mHag allele positive or negative (indicated as ACC-1$^{C}$); **b** cytotoxic activity of the HLA-A*0201-restricted, HA-1$^{H}$-specific EH6-CTL clone against HLA-A*0201-positive dermal fibroblasts and B-LCLs that were either HA-1$^{H}$ mHag allele positive or negative (indicated as HA-1$^{R}$). IFN-$\gamma$ + TNF-$\alpha$ treatment was performed as described in Fig. 3. The effector target ratio was fixed at 30:1

demonstrated promising results [20–22]. After allogeneic HSCT for patients with melanoma, there have been some reports indicating that CTLs against melanoma cells do exist and that these melanoma-reactive CTLs can be expanded in vitro [23, 24]. These observations suggest that allogeneic HSCT after a nonmyeloablative conditioning regimen might be a promising therapeutic strategy for patients with refractory metastatic melanoma.

Childs et al., however, reported relatively disappointing results in which 5 out of 11 metastatic melanoma patients receiving allogeneic HSCT died from rapid tumor growth, while the rest of the patients showed variable results [14]. As in the case of hematological malignancies, a high tumor burden should be one of the most unfavorable factors regarding treatment failure with allogeneic HSCT. Therefore, a treatment strategy combining the selection of patients with a lower tumor burden or slower growth kinetics and allogeneic HSCT may be explored for this poor-prognosis disease if the given donor and recipient are eligible for immunotherapy using ACC-1 and ACC-2 mHags, or other hematopoiesis-specific mHags are also highly expressed in melanoma cells. Since HSCT recipients eligible for ACC-1, ACC-2, and HA-1 mHags exist at a frequency of 11, 3, and 9%, respectively, in Japanese [25], it would be possible to apply these mHags to nearly a quarter of such patients.

BCL2A1 is a member of the B-cell lymphoma-2 (BCL2) family. *BCL2* is highly expressed in melanoma, which was shown to contribute to a chemoresistant phenotype [26]. The reduction of BCL2 by siRNA caused melanoma cells to become susceptible to chemotherapeutic agents. BCL2A1, although regulated differently from BCL2, also exerts antiapoptotic activity and is expressed even in normal melanocytes like other melanocyte differentiating antigens, such as Melan-A/MART-1 or tyrosinase. In this regard, BCL2A1 would be essential for melanoma cells and melanocyte survival, suggesting that it may be a good candidate antigen for immunotherapy against melanoma, although autoimmune depigmentation may also develop, as seen in adoptive immunotherapy targeting melanoma-associated antigens mentioned above [20, 21].

In addition, we unexpectedly found that, after cytokine treatment, dermal fibroblasts upregulated both *BCL2A1* and *HMHA1* expression and become susceptible to cognate CTL clones, respectively (Fig. 4). This suggests that, after allogeneic HSCT, they would also be upregulated under a "cytokine-storm", and may contribute in some way to the pathophysiology of skin GVHD. In the clinical setting, HA-1 was originally reported as an mHag associated with GVHD [27], and additional studies brought about mixed results, making it still too early to draw any conclusion [28, 29], while ACC-1$^{Y}$ disparity did not seem to be associated with an increased incidence of acute GVHD [30]. In skin explant assays, it was shown that skin sections from HLA-A2$^{+}$ HA-1$^{+}$ individuals incubated with HA-1 CTLs developed only background grade I or low grade II GVH reactions, while male HLA-A2$^{+}$ skin sections incubated with Y antigen-specific CTLs displayed severe GVH reactions of grade III–IV [31]. It is assumed that stronger GVH reactions might be observed if skin sections are pretreated with cytokines before incubation with HA-1-specific CTLs. IFN-$\gamma$, which is known to induce various transcription factors specific for hematopoiesis and immunity, might be a key in this upregulation of hematopoietic cell-restricted mHags in dermal fibroblasts. Since IFN-$\gamma$ is strongly produced by CTLs and type 1 helper T cells, the IFN-$\gamma$ secreted from mHag-specific CTLs could lead to the upregulation of target hematopoiesis-specific

mHags, resulting in GVHD or GVT effects in tumors sensitive to the IFN-γ-induced upregulation of such mHags. Therefore, it is crucial to develop a new treatment strategy to induce selective GVT effects while avoiding life-threatening GVHD using preconditioning and GVHD prophylaxis regimens to minimize GVHD, followed by selective immunotherapy targeting mHags mainly expressed in tumors and hematopoietic cells, such as ACC-1, -2, and HA-1, after the "cytokine storm" period is over.

In summary, *BCL2A1*-encoded mHags, ACC-1 and ACC-2, may be potential targets of immunological interventions for a fraction of patients with refractory, but not bulky melanoma following allogeneic HSCT.

## References


1. den Haan JM, Meadows LM, Wang W, et al. The minor histocompatibility antigen HA-1: a diallelic gene with a single amino acid polymorphism. Science. 1998;279:1054–7.
2. Kawase T, Akatsuka Y, Torikai H, et al. Alternative splicing due to an intronic SNP in HMSD generates a novel minor histocompatibility antigen. Blood. 2007;110:1055–63.
3. Bleakley M, Riddell SR. Molecules and mechanisms of the graft-versus-leukaemia effect. Nat Rev Cancer. 2004;4:371–80.
4. Atkins MB, Lotze MT, Dutcher JP, et al. High-dose recombinant interleukin 2 therapy for patients with metastatic melanoma: analysis of 270 patients treated between 1985 and 1993. J Clin Oncol. 1999;17:2105–16.
5. McDermott DF. Update on the application of interleukin-2 in the treatment of renal cell carcinoma. Clin Cancer Res. 2007;13:716s–20s.
6. Ravaud A, Dilhuydy MS. Interferon alpha for the treatment of advanced renal cancer. Expert Opin Biol Ther. 2005;5:749–62.
7. Bishop MR, Fowler DH, Marchigiani D, et al. Allogeneic lymphocytes induce tumor regression of advanced metastatic breast cancer. J Clin Oncol. 2004;22:3886–92.
8. Childs R, Chernoff A, Contentin N, et al. Regression of metastatic renal-cell carcinoma after nonmyeloablative allogeneic peripheral-blood stem-cell transplantation. N Engl J Med. 2000;343:750–8.
9. Klein CA, Wilke M, Pool J, et al. The hematopoietic system-specific minor histocompatibility antigen HA-1 shows aberrant expression in epithelial cancer cells. J Exp Med. 2002;196:359–68.
10. Fujii N, Hiraki A, Ikeda K, et al. Expression of minor histocompatibility antigen, HA-1, in solid tumor cells. Transplantation. 2002;73:1137–41.
11. Miyazaki M, Akatsuka Y, Nishida T, et al. Potential limitations in using minor histocompatibility antigen-specific cytotoxic T cells for targeting solid tumor cells. Clin Immunol. 2003;107:198–201.
12. Slager EH, Honders MW, van der Meijden ED, et al. Identification of the angiogenic endothelial-cell growth factor-1/thymidine phosphorylase as a potential target for immunotherapy of cancer. Blood. 2006;107:4954–60.
13. Akatsuka Y, Nishida T, Kondo E, et al. Identification of a polymorphic gene, BCL2A1, encoding two novel hematopoietic lineage-specific minor histocompatibility antigens. J Exp Med. 2003;197:1489–500.
14. Childs R, Srinivasan R. Advances in allogeneic stem cell transplantation: directing graft-versus-leukemia at solid tumors. Cancer J. 2002;8:2–11.
15. Su AI, Cooke MP, Ching KA, et al. Large-scale analysis of the human and mouse transcriptomes. Proc Natl Acad Sci USA. 2002;99:4465–70.
16. Kloosterboer FM, van Luxemburg-Heijs SA, van Soest RA, van Egmond HM, Willemze R, Falkenburg JH. Up-regulated expression in nonhematopoietic tissues of the BCL2A1-derived minor histocompatibility antigens in response to inflammatory cytokines: relevance for allogeneic immunotherapy of leukemia. Blood. 2005;106:3955–7.
17. Khammari A, Nguyen JM, Pandolfino MC, et al. Long-term follow-up of patients treated by adoptive transfer of melanoma tumor-infiltrating lymphocytes as adjuvant therapy for stage III melanoma. Cancer Immunol Immunother. 2007;56:1853–60.
18. Boon T, Coulie PG, Van den Eynde BJ, van der Bruggen P. Human T cell responses against melanoma. Annu Rev Immunol. 2006;24:175–208.
19. Machiels JP, van Baren N, Marchand M. Peptide-based cancer vaccines. Semin Oncol. 2002;29:494–502.
20. Yee C, Thompson JA, Byrd D, et al. Adoptive T cell therapy using antigen-specific CD8+ T cell clones for the treatment of patients with metastatic melanoma: in vivo persistence, migration, and antitumor effect of transferred T cells. Proc Natl Acad Sci USA. 2002;99:16168–73.
21. Dudley ME, Wunderlich JR, Robbins PF, et al. Cancer regression and autoimmunity in patients after clonal repopulation with antitumor lymphocytes. Science. 2002;298:850–4.
22. Dudley ME, Wunderlich JR, Yang JC, et al. Adoptive cell transfer therapy following non-myeloablative but lymphodepleting chemotherapy for the treatment of patients with refractory metastatic melanoma. J Clin Oncol. 2005;23:2346–57.
23. Kurokawa T, Fischer K, Bertz H, Hoegerle S, Finke J, Mackensen A. In vitro and in vivo characterization of graft-versus-tumor responses in melanoma patients after allogeneic peripheral blood stem cell transplantation. Int J Cancer. 2002;101:52–60.
24. Gottlieb DJ, Li YC, Lionello I, et al. Generation of tumour-specific cytotoxic T-cell clones from histocompatibility leucocyte antigen-identical siblings of patients with melanoma. Br J Cancer. 2006;95:181–8.
25. Akatsuka Y, Morishima Y, Kuzushima K, Kodera Y, Takahashi T. Minor histocompatibility antigens as targets for immunotherapy using allogeneic immune reactions. Cancer Sci. 2007;98:1139–46.
26. Vlaykova T, Talve L, Hahka-Kemppinen M, et al. Immunohistochemically detectable bcl-2 expression in metastatic melanoma: association with survival and treatment response. Oncology. 2002;62:259–68.
27. Goulmy E, Schipper R, Pool J, et al. Mismatches of minor histocompatibility antigens between HLA-identical donors and recipients and the development of graft-versus-host disease after bone marrow transplantation. N Engl J Med. 1996;334:281–5.
28. Tseng LH, Lin MT, Hansen JA, et al. Correlation between disparity for the minor histocompatibility antigen HA-1 and the development of acute graft-versus-host disease after allogeneic marrow transplantation. Blood. 1999;94:2911–4.
29. Murata M, Emi N, Hirabayashi N, et al. No significant association between HA-1 incompatibility and incidence of acute graft-versus-host disease after HLA-identical sibling bone marrow transplantation in Japanese patients. Int J Hematol. 2000;72:371–5.
30. Nishida T, Akatsuka Y, Morishima Y, et al. Clinical relevance of a newly identified HLA-A24-restricted minor histocompatibility antigen epitope derived from BCL2A1, ACC-1, in patients receiving HLA genotypically matched unrelated bone marrow transplant. Br J Haematol. 2004;124:629–35.
31. Dickinson AM, Wang XN, Sviland L, et al. In situ dissection of the graft-versus-host activities of cytotoxic T cells specific for minor histocompatibility antigens. Nat Med. 2002;8:410–4.

Int J Hematol (2008) 88:311–320
DOI 10.1007/s12185-008-0134-z

ORIGINAL ARTICLE

# CD137-guided isolation and expansion of antigen-specific CD8 cells for potential use in adoptive immunotherapy

**Kazue Watanabe · Susumu Suzuki · Michi Kamei · Shingo Toji · Takakazu Kawase · Toshitada Takahashi · Kiyotaka Kuzushima · Yoshiki Akatsuka**

Received: 20 September 2007 / Revised: 7 May 2008 / Accepted: 9 June 2008 / Published online: 5 August 2008


**Abstract** The efficient isolation and ex vivo expansion of antigen-specific T cells are crucial for successful adoptive immunotherapy against uncontrollable infections and cancers. Several methods have been reported for this purpose, for example, employing MHC-multimeric complexes, interferon-gamma secretion, and antibodies specific for molecules expressed on T-cell surfaces, including CD25, CD69, CD107a, CD137, and CD154. Of the latter, CD137 has been shown to be one of the most promising targets since it is only expressed on $CD8^+$ T cells early after encountering antigen, while being almost undetectable on resting cells. However, detailed comparisons between CD137-based and other methods have not yet been conducted. In this study, we therefore compared three approaches (with CD137, CD107a, and tetramers) using HLA-A24-restricted CMV pp65 and EBV BRLF1 epitopes as model antigens. We found that the CD137-based isolation of antigen-stimulated $CD8^+$ T cells was comparable to tetramer-based sorting in terms of purity and superior to the other two methods in terms of subsequent cell expansion. The method was less applicable to $CD4^+$ T cells since their CD137 upregulation is not sufficiently high. Collectively, this approach is most likely to be optimal among the methods tested for the isolation and expansion of antigen-specific $CD8^+$ cells.

**Keywords** CD137 · Adoptive transfer · Cytotoxic T lymphocyte · Sorting

K.W. and S.T. are employees of Medical Biological Laboratories Co., Ltd. S.S. is a representative executive of T Cell Technologies, Inc. Y.A. has received financial support through collaboration with Medical Biological Laboratories Co., Ltd.

K. Watanabe (✉) · S. Toji
Research Reagent Division, Medical Biological Laboratories Co., Ltd., 1063-103 Ohara, Terasawaoka, Ina, Nagano 396-0002, Japan
e-mail: watanabe.kazue@mbl.co.jp

K. Watanabe · M. Kamei · T. Kawase · T. Takahashi · K. Kuzushima · Y. Akatsuka (✉)
Division of Immunology, Aichi Cancer Center Research Institute, 1-1 Kanokoden, Chikusa-ku, Nagoya, Aichi 464-8681, Japan
e-mail: yakatsuk@aichi-cc.jp

S. Suzuki
T Cell Technologies, Inc., 3-5-10 Marunouchi, Naka-ku, Nagoya 460-0002, Japan

M. Kamei
Department of Pediatrics and Neonatology, Nagoya City University, Graduate School of Medical Science, Nagoya, Japan

K. Kuzushima
Department of Cellular Oncology, Nagoya University Graduate School of Medicine, Nagoya, Japan

## 1 Introduction

Patients under severe immunosuppression after organ transplantation or chemotherapy, or due to congenital/acquired immunodeficiency, are vulnerable to infections with viruses such as cytomegalovirus (CMV) and Epstein–Barr virus (EBV), which are major causes of morbidity and mortality. Although the advent of new antiviral drugs for CMV [1] or anti-CD20 antibodies for EBV-associated B cell malignancies [2] has improved the survival of patients at risk, the adoptive transfer of T cells specific for these viruses still remains an attractive strategy, especially when the viruses or virus-associated tumors are resistant to such agents [3]. The powerful antiviral effects of infused T cells have been reported in various clinical settings [4–6]. There

are two ways to compensate for immunodeficiency in patients: (1) the infusion of ex vivo-expanded viral antigen-specific T cells; and (2) direct transfusion of peripheral blood T cells from healthy donors when the patients receive allogeneic hematopoietic cell transplantation. Although the latter method is feasible, there is a risk of graft versus host disease and it usually takes at least a few weeks before antiviral T cells have effectively expanded in vivo [7]. In contrast, although the former method is cumbersome and also time-consuming one at the ex vivo step, it is expected to be more effective and safer since only armed and selected viral antigen-specific T cells are infused [8].

Recently, several methods to detect and positively sort T cells specific for antigens of interest have been reported. These include the sorting of T cells stained with peptide/MHC multimers, with antibodies that react to cell surface-exposed CD107 (LAMP1) [9, 10], cell surface-captured interferon-gamma (IFN-$\gamma$), with the aid of a special biphasic antibody [11], and CD137 [12] as a more antigen-specific activation marker than CD25 or CD69. Except in tetramer or multimer cases, T cells activated with whole antigen without prior knowledge of the restriction HLA alleles or epitopes have been shown to be positively selected by flow-sorting or with magnetic beads using any of the above-mentioned methods. As these methods are based on the specific functions of individual cells, it is not easy to determine which method is most feasible for routine immunological studies and clinical application. In this report, we compared the results using three methods (using tetramers, CD107a, and CD137), all of which require a single staining step, employing CMV pp65 and EBV BRLF1 epitopes as model antigens, focusing on their merits and limitations.

## 2 Materials and methods

### 2.1 Cells and culture media

Peripheral blood mononuclear cells (PBMCs) were isolated by centrifugation on a Ficoll density gradient. All blood samples were collected after obtaining written informed consent, and the study was approved by the institutional review board of Aichi Cancer Center. Primary T cell lines were induced in RPMI 1640 (Sigma–Aldrich, St. Louis, MO, USA) supplemented with 12.5 mM HEPES, 5% autologous plasma, penicillin/streptomycin, and 2 mM L-glutamine (referred to as T cell medium). Epstein–Barr virus-transformed B cells (B-LCL) were established by infecting an aliquot of PBMCs with B95-8 supernatant.

### 2.2 Antibodies, tetramers, and flow cytometric analysis

Antibodies used for sorting and phenotyping were as follows: anti-CD4-PC5, anti-CD8-PC5, anti-CD28-PE, anti-CD45RA-PE, anti-CD45RO-FITC (all from Beckman Coulter Inc., Miami, FL, USA) anti-CD137-FITC (MBL, Nagoya, Japan), anti-CD107a-FITC (Southern Biotech, Birmingham, AL, USA), anti-CD137-PE (BD Biosciences, San Diego, CA, USA), and anti-CCR7-FITC (R&D systems, Minneapolis, MN, USA). For intracellular interferon (IFN)-$\gamma$ staining, anti-IFN-$\gamma$-FITC was from MBL (Nagoya, Japan). HLA-A*2402 CMVpp65, HLA-A*0201 CMV pp65, HLA-A*2402 EBV-BRLF1, and HLA-DRB1*0101 EBNA1 tetramers were purchased from MBL (Nagoya, Japan). Cells were first stained with tetramers for 15 min at room temperature, and then stained with appropriate combinations of antibodies for 15 min on ice. Flow cytometric analysis of the cells was performed using a FACSCalibur (BD Biosciences) with the aid of CellQuest software (BD Biosciences).

### 2.3 Peptides

The following peptides were synthesized by BioSynthesis (Lewisville, TX, USA): CMV/pp65(341–349) (QYDPVAALF, referred to as CMV-QYD hereafter), CMV/pp65(495–503) (NLVPMVATV, as CMV-NLV), EBV/BRLF1(320–328) (DYNFVKQLF, as EBV-DYN), and EBV/EBNA1(515–527) (TSLYNLRRGTALA, as EBV-TSL).

### 2.4 Induction of T cell lines by mixed lymphocyte-peptide cultures (MLPCs) (Fig. 1a)

The antigenic peptides listed above were directly added to PBMCs at 10 μg/ml suspended in 2 ml T cell medium in a 15-ml round-bottomed tube (BD Biosciences), and the cultures were maintained at 37°C and 5% $CO_2$. On day 2, recombinant human IL-2 (50 U/ml, Shionogi Pharmaceutical Institute Co., Osaka, Japan) was added. Starting on day 5, half-medium change and supplementation of IL-2 were performed every other day until day 14.

### 2.5 Restimulation and positive selection of antigen-specific T cells

Restimulation of MLPC T cell lines for the analysis of CD107a and CD137 expression followed by positive selection with MACS beads was performed 14 days after the primary stimulation. The optimal peptide concentration was predetermined for individual epitopes. Peptide was directly added to the aliquot of T cell lines without any antigen-presenting cells (APCs) and cytokines. For the determination of the optimal timing for positive selection either with anti-CD107a, or anti-CD137 antibody, the expression of CD107 and CD137 on antigen-specific T cells (identified by cognate tetramer) was assessed at

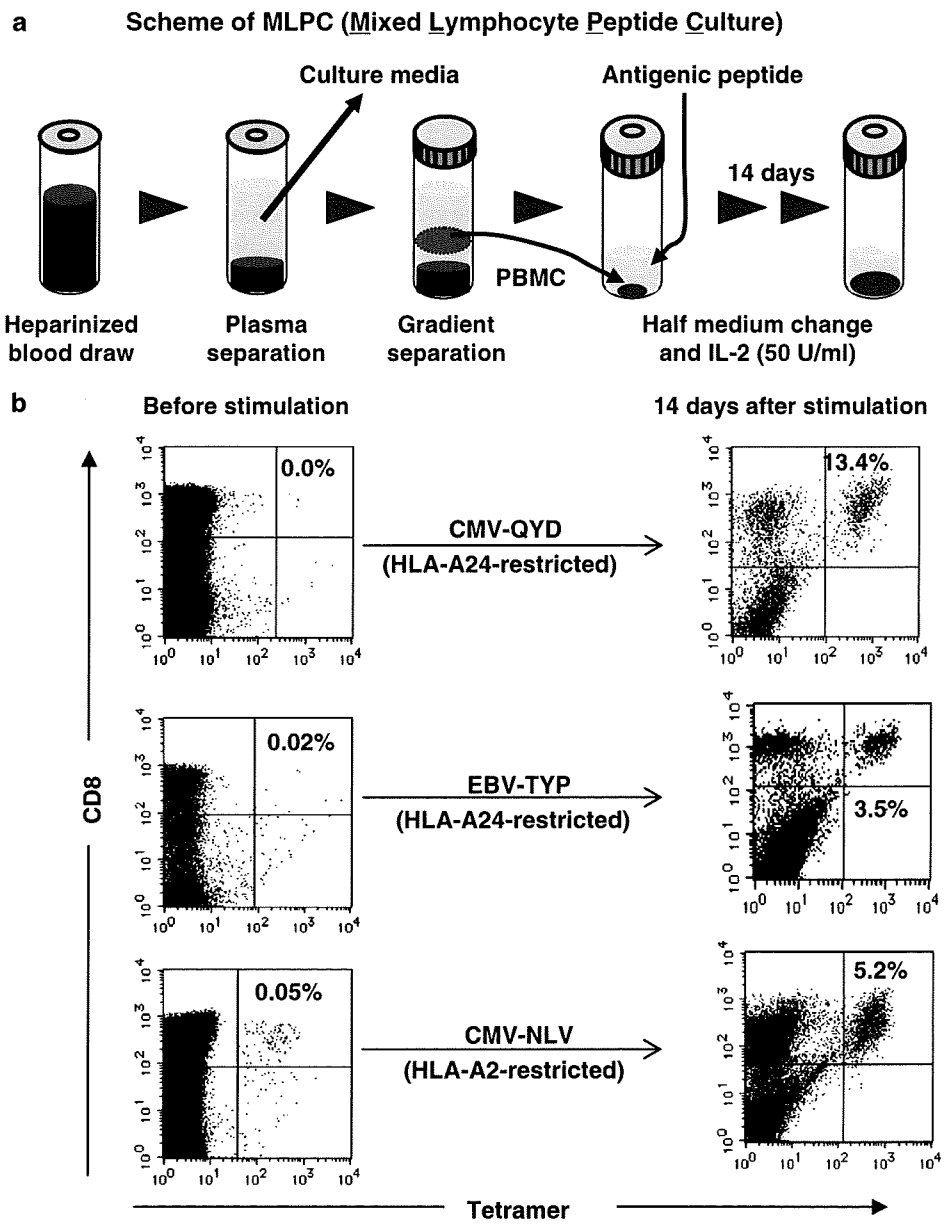


**Fig. 1** **a** Schematic diagram of mixed lymphocyte peptide culture (MLPC). Heparinized whole blood was first centrifuged to obtain plasma for culture media preparation. Peripheral blood mononuclear cells (PBMCs) were then separated by density gradient centrifugation from the resuspended blood pellets and cultured in RPMI1640 medium supplemented with 5% autologous plasma in the presence of 10 μg/ml of antigenic peptide for 14 days. **b** Induction of viral antigen-specific T cell lines by MLPC. PBMCs were stained with the indicated tetramer before and after stimulation with the corresponding peptide. The percentages of tetramer$^+$ cells among CD3$^+$ populations are indicated. The data shown are representative of the following numbers of experiments: CMV-QYD, $n = 17$; EBV-TYP, $n = 10$; CMV-NLV, $n = 5$

various time points. After incubation for the predetermined time, T cell lines were washed and stained with either FITC-labeled CD107a, or CD137 antibody at 10 μg/ml in PBS containing 0.5% human serum albumin for 15 min at 4°C. After washing with MACS buffer (phosphate-buffered saline supplemented with 0.5% human serum albumin and 2 mM EDTA), the cells were incubated with anti-murine IgG1 MACS beads (Miltenyi Biotec, Auburn, CA, USA) for 15 min at 4°C. Cell separation was conducted using AutoMACS (Miltenyi Biotec). Antigen-specific T cells were also isolated without prior antigenic stimulation using cognate PE-conjugated tetramers followed by separation with anti-PE MACS beads and AutoMACS.

### 2.6 Expansion of sorted antigen-specific T cells

Sorted T cells were propagated in appropriately sized culture vessels in ALyS505N-1000 medium (Cell Science & Technology Institute, Inc., Sendai, Japan) originally containing 1000 U/ml of IL-2. Cultures were fed by changing half of the supernatant twice a week.

### 2.7 CFSE-based cytotoxicity assay

Target B-LCLs were labeled with 1 μM 6-carboxyfluorescein diacetate succinimidyl ester (CFSE; Wako Pure Chemical Industry, Osaka, Japan) for 10 min at 25°C.

After two washes, the CFSE-labeled target cells were cocultured with graded numbers of effector T cells for 5 h at 37°C and 5% $CO_2$ in the presence or absence of peptides in 96-well microtiter plates. The whole cells were harvested and stained with Annexin-V and Kusabira Orange (MBL) for 15 min at 25°C according to the manufacturer's instructions, and the absolute number of surviving cells was determined using a FACSCalibur with the aid of CellQuest software. The percentage lysis was calculated as follows:

$$[(ET - T0)/(100 - T0)] \times 100.$$

ET indicates percentage of $CFSE^+$ Annexin-$V^+$ target cells cocultured with effector cells, and T0 indicates the percentage of $CFSE^+$ Annexin-$V^+$ target cells without effector cells.

### 2.8 Statistical analysis

Data were expressed as the average ± SD of seven experiments. Samples were compared by paired Student's *t* test analyses using on-line software available at http://www.physics.csbsju.edu/stats/t-test.html.

## 3 Results

### 3.1 Induction of viral antigen-specific T cell lines by MLPC

We first sought to determine whether a simple MLPC could expand cognate antigen-specific T cells from healthy donors serologically positive for CMV and/or EBV (Fig. 1a). As shown in Fig. 1b, 3–15% of $CD8^+$ $tetramer^+$ populations among surviving cells with the cultured PBMCs were readily obtained after 14 days of culture, although the magnitude of responses varied depending on the epitope peptides and donors. The induction of T cells from seronegative donors was not attempted.

### 3.2 Kinetics of CD107a and CD137 expression following stimulation

It is important to determine when the activation markers are maximally upregulated for optimal sorting. Although CD137 expression kinetics have been reported elsewhere [12], we made a comparison with those of CD107a. As shown in Fig. 2a, CD137 expression among $tetramer^+$ cells exceeded 90% around 16 h following stimulation with the predetermined minimal concentration (10 ng/ml, see below) of CMV-QYD peptide. The expression started to decline after 24 h, and only 25% of the cells remained positive after 48 h. In the case of CD107a, upregulation was much quicker than with CD137, and a 70% level was maintained between 4 and 24 h, followed by a decline to 25% after 48 h. The maximal CD107a expression level was around 20% lower than that of CD137, and, unexpectedly, CD107a molecules exposed by the degranulation of CTLs remained on outer membranes for up to 24 h. Thus, we decided to perform the following positive selection experiments around 20 h after antigenic stimulation.

### 3.3 Optimization of peptide and primary antibody concentrations

Excessive antigenic stimulation is known to cause activation-induced cell death (AICD) in T cells [13]; thus, it is important to determine the minimal peptide concentration which results in sufficient CD137 expression. In the case of HLA-A24-restricted CMV-QYD peptide, the minimal concentration required to obtain more than 90% $CD137^+$ cells among the cognate $tetramer^+$ population was 10 ng/ml, and the use of 100 ng/ml resulted in a significant reduction of live cells, possibly due to AICD (Fig. 2b, c and data not shown). The optimal peptide concentrations differed among peptides; for example, 1 ng/ml was sufficient for the HLA-A24-restricted EBV-TYP peptide (data not shown), suggesting that the predetermination of optimal concentrations for individual peptides is necessary. A similar trend was observed when the extent of degranulation was assessed with CD107a antibody (data not shown).

The CD137 antibody (clone 4B4-1) itself does not induce AICD, but we also sought to determine sufficient concentrations by titration with measurement of the mean fluorescence intensity. In most cases, sufficient staining was obtained around 10 μg/ml (Fig. 2d and data now shown), which is a commonly employed concentration in most cell-staining procedures. Thus, we decided to use this concentration throughout the following experiments.

### 3.4 Comparison of three positive selection methods

Figure 3a shows the schematic procedures to positively select antigen-specific T cells by CD137, CD107a, or tetramer staining followed by MACS-based capture. In the case of tetramer-based sorting, peptide stimulation was not performed prior to sorting because it led to diminished tetramer staining, possibly due to the downregulation of T cell receptors (TCRs) on cognate T cells (upper right panel of Fig. 3b). The marked difference observed in sorted fractions just after positive selection was due to the fact that the tetramer-sorted fraction contained an average of 93% $CD8^+$ $tetramer^+$ cells (Table 1), while those obtained by CD107a and to lesser extent CD137 methods contained substantial numbers of $tetramer^-$ cells (Fig. 3b, second panel from the top). Since the $tetramer^-$ fractions were

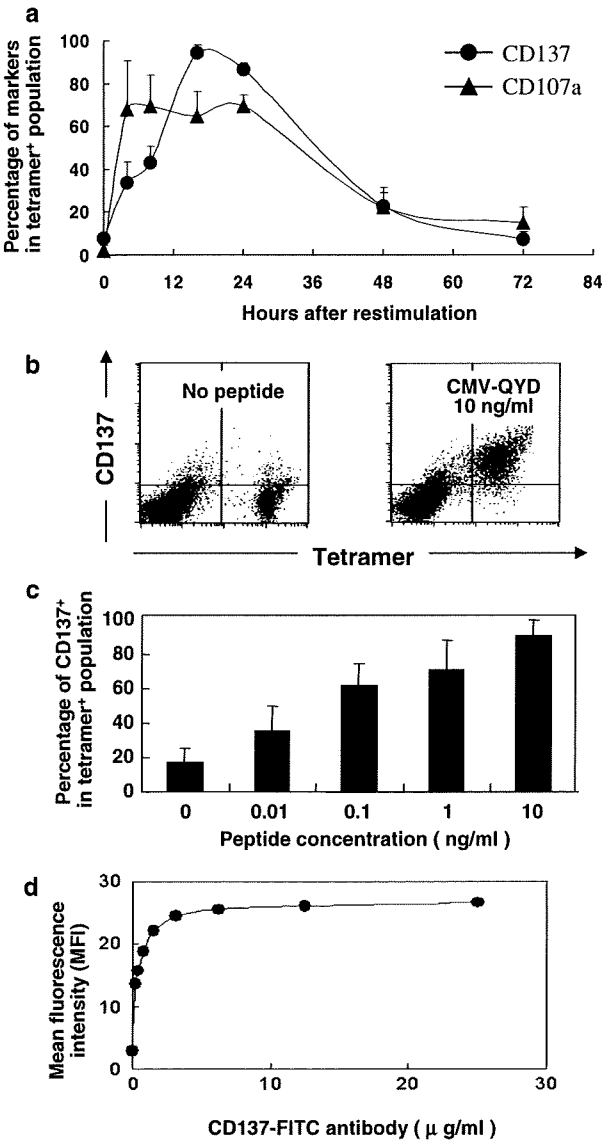


**Fig. 2** Optimization of conditions for positive selection. **a** Expression kinetics of CD137 and CD107a on T cells generated by MLPC with the CMV-QYD peptide. The percentages of indicated marker (CD137 or CD107a)-positive cells among tetramer$^+$ T cell populations after stimulation with 10 ng/ml CMV-QYD peptide are longitudinally plotted. The data shown are mean and SD values from four independent experiments. **b** A representative profile of CD137 expression before and after stimulation with the CMV-QYD peptide. **c** Titration of the CMV-QYD peptide for the full upregulation of CD137. T cell lines generated by MLPC with CMV-QYD peptide were restimulated with the indicated concentrations of peptide, and the percentages of CD137$^+$ cells among the tetramer$^+$ population were plotted. The data shown are mean and SD values from five independent experiments. **d** Titration of CD137 antibodies. The mean fluorescence intensity (MFI) of CD137 staining with graded concentrations of FITC-conjugated CD137 antibodies is shown. T cell lines were the same as used in **c** and were stimulated with 10 ng/ml CMV-QYD peptide for CD137 upregulation

composed of both CD8$^+$ and CD4$^+$ cells, it is likely that these fractions came from T cells that expressed CD137 or CD107a molecules nonspecifically. Antigen-independent, spontaneous CD137 upregulation in tetramer$^-$ cells was indeed present (Fig. 2b), which might explain the recovery of tetramer$^-$ cells by CD137- and CD107a-based sorting. However, following culture for 7 days, these tetramer$^-$ cells showed a trend toward disappearance, suggesting either the loss of the growth of cells that had been expressing CD137/CD107a non-relevant to antigen stimulation, or relative outgrowth of antigen-specific cells after sorting (Fig. 3b, bottom panels and Table 1).

Data regarding the recovery of CMV-QYD-specific T cells with the three sorting methods are summarized in Table 1. Due to a consistently high percentage (average >93%) of tetramer$^+$ cells in the tetramer-sorted fraction, the total recovery of tetramer$^+$ cells was also constant (34–44.5%). In Experiment 3, however, the poor cell recovery, especially with CD107a-based sorting using the AutoMACS device, was most likely caused by unexpectedly low CD107a induction (11.3% among tetramer$^+$ cells). Nevertheless, in the other two experiments, both CD137- and CD107a-based methods resulted in a better recovery of tetramer$^+$ cells than the tetramer-based method.

We next sought to determine which method was most suitable for expanding enriched antigen-specific T cells after sorting. Fig. 4a and b shows the growth kinetics of sorted fractions cultured in the presence of IL-2, but without any feeder cells for T cell lines specific for CMV-QYD (Fig. 4a) and EBV-TYP (Fig. 4b) obtained from seven individuals. In the CMV-QYD group, T cell lines enriched with the CD137-based method readily showed significantly better growth than those enriched with tetramer (Fig. 4a). In the EBV-TYP group, T cell lines enriched with the CD137-based method showed a trend toward better growth than those enriched with tetramer ($P = 0.084$ for day 7 and $P = 0.063$ for day 14, Fig. 4b). In the case of T cell lines enriched with CD107a, those specific for CMV-QYD showed moderate growth (Fig. 4a), while those specific for EBV-TYP remained unchanged in number (Fig. 4b). The difference of growth kinetics did not reach significance for CD137-based versus CD107a-based methods; however, there was a constant trend toward an increased number of antigen-specific T cells among the CD137-based sorting group (Fig. 4a, b).

### 3.5 Phenotype and functional aspects of T cell lines sorted by CD137

Since CD137-based enrichment gave promising results, especially with expansion after sorting, we further